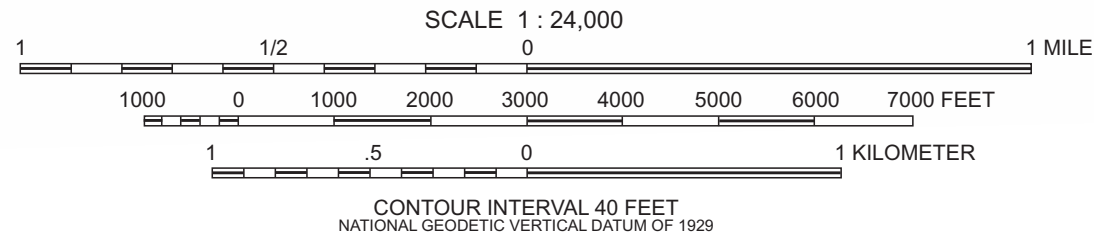
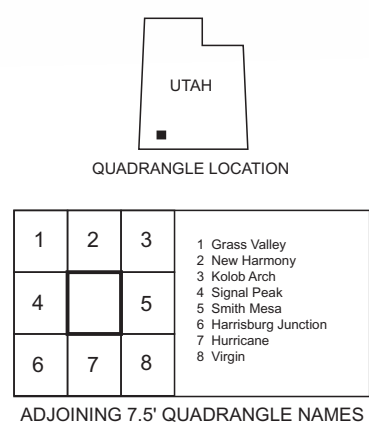


The views and conclusions contained in this document are those of the authors and should not be interpreted as necessarily representing the official policies, either expressed or implied, of the U.S. Government.



## by







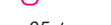








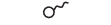





2003



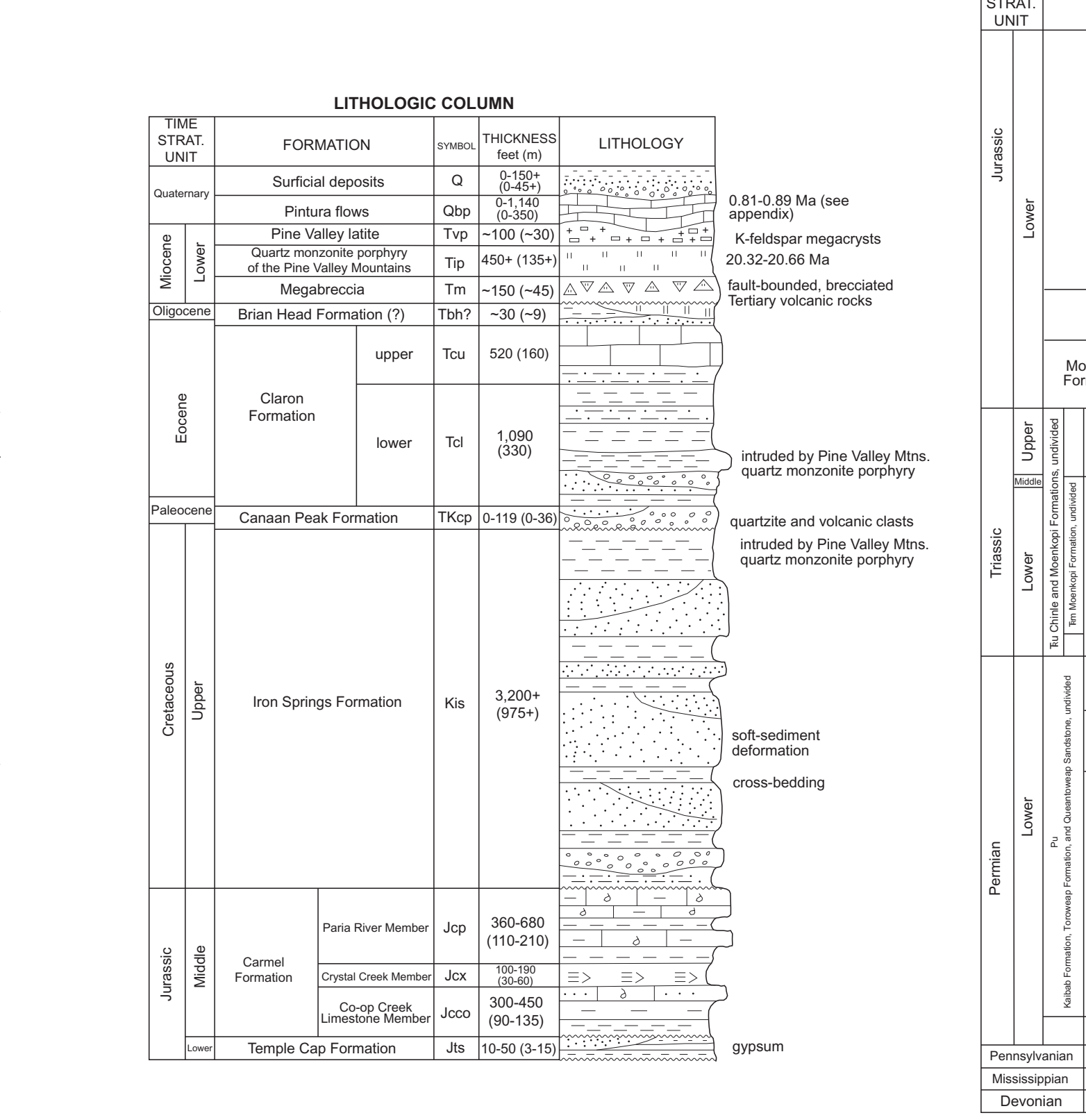


### DESCRIPTION OF MAP UNITS

Research funded by the Utah Geological Survey  
and the U.S. Geological Survey National  
Cooperative Geologic Mapping Program, through  
USGS STATEMAP award number 99HQAG0138.

MAP SYMBOLS	
	Contact
	High-angle normal fault, dashed where approximately located, dotted where concealed; bar and ball on down-thrown side; arrow indicates dip of exposed fault surface
	Low-angle normal fault; open teeth on upper plate
	Thrust fault, dotted where concealed, queried where uncertain; teeth on upper plate
	Axial trace of anticline, showing direction of plunge; dashed where approximately located, dotted where concealed
	Axial trace of syncline
	Axial trace of overturned syncline
	Strike and dip of inclined bedding
	Approximate strike and dip of inclined bedding determined from aerial photography
	Approximate strike and dip direction of inclined bedding
	Strike of vertical bedding
	Strike and dip of overturned bedding
	Pit - sand and gravel
	Quarry
	Prospect
	Mine shaft
	Spring (see also figure 3 and table 2)
	Water well (see also figure 3 and table 1)
	Petroleum exploration drill hole - plugged and abandoned (see also table 3)
	Sinkhole
	Sample location and number

### CORRELATION OF QUATERNARY UNITS





# GEOLOGIC MAP OF THE PINTURA QUADRANGLE, WASHINGTON COUNTY, UTAH

*by*

*Hugh A. Hurlow and Robert F. Biek*

This geologic map was funded by the Utah Geological Survey and the U.S. Geological Survey, National Cooperative Geologic Mapping Program through STATEMAP Agreement No. 99HQAG0138

Although this product represents the work of professional scientists, the Utah Department of Natural Resources, Utah Geological Survey, makes no warranty, expressed or implied, regarding its suitability for a particular use. The Utah Department of Natural Resources, Utah Geological Survey, shall not be liable under any circumstances for any direct, indirect, special, incidental, or consequential damages with respect to claims by users of this product.

The views and conclusions contained in this document are those of the authors and should not be interpreted as necessarily representing the official policies, either expressed or implied, of the U.S. Government.

ISBN 1-55791-596-2



**MAP 196**  
**Utah Geological Survey**  
*a division of*  
Utah Department of Natural Resources



**STATE OF UTAH**  
*Olene S. Walker, Governor*

**DEPARTMENT OF NATURAL RESOURCES**  
*Robert Morgan, Executive Director*

**UTAH GEOLOGICAL SURVEY**  
*Richard G. Allis, Director*

**UGS Board**

<b>Member</b>	<b>Representing</b>
Robert Robison (Chairman) .....	Minerals (Industrial)
Geoffrey Bedell .....	Minerals (Metals)
Stephen Church .....	Minerals (Oil and Gas)
Kathleen Ochsenbein .....	Public-at-Large
Craig Nelson .....	Engineering Geology
Charles Semborski .....	Minerals (Coal)
Ronald Bruhn .....	Scientific
Kevin Carter, Trust Lands Administration .....	<i>Ex officio member</i>

**UTAH GEOLOGICAL SURVEY**

The **UTAH GEOLOGICAL SURVEY** is organized into five geologic programs with Administration and Editorial providing necessary support to the programs. The **ENERGY & MINERAL RESOURCES PROGRAM** undertakes studies to identify coal, geothermal, uranium, hydrocarbon, and industrial and metallic resources; initiates detailed studies of these resources including mining district and field studies; develops computerized resource data bases, to answer state, federal, and industry requests for information; and encourages the prudent development of Utah's geologic resources. The **GEOLOGIC HAZARDS PROGRAM** responds to requests from local and state governmental entities for engineering-geologic investigations; and identifies, documents, and interprets Utah's geologic hazards. The **GEOLOGIC MAPPING PROGRAM** maps the bedrock and surficial geology of the state at a regional scale and at a more detailed scale by quadrangle. The **GEOLOGIC INFORMATION & OUTREACH PROGRAM** answers inquiries from the public and provides information about Utah's geology in a non-technical format. The **ENVIRONMENTAL SCIENCES PROGRAM** maintains and publishes records of Utah's fossil resources, provides paleontological and archeological recovery services to state and local governments, conducts studies of environmental change to aid resource management, and evaluates the quantity and quality of Utah's ground-water resources.

The UGS Library is open to the public and contains many reference works on Utah geology and many unpublished documents on aspects of Utah geology by UGS staff and others. The UGS has several computer databases with information on mineral and energy resources, geologic hazards, stratigraphic sections, and bibliographic references. Most files may be viewed by using the UGS Library. The UGS also manages the Utah Core Research Center which contains core, cuttings, and soil samples from mineral and petroleum drill holes and engineering geology investigations. Samples may be viewed at the Utah Core Research Center or requested as a loan for outside study.

The UGS publishes the results of its investigations in the form of maps, reports, and compilations of data that are accessible to the public. For information on UGS publications, contact the Natural Resources Map/Bookstore, 1594 W. North Temple, Salt Lake City, Utah 84116, (801) 537-3320 or 1-888-UTAH MAP. E-mail: [geostore@utah.gov](mailto:geostore@utah.gov) and visit our web site at <http://mapstore.utah.gov>.

**UGS Editorial Staff**

J. Stringfellow .....	Editor
Vicky Clarke, Sharon Hamre.....	Graphic Artists
James W. Parker, Lori Douglas .....	Cartographers

---

*The Utah Department of Natural Resources receives federal aid and prohibits discrimination on the basis of race, color, sex, age, national origin, or disability. For information or complaints regarding discrimination, contact Executive Director, Utah Department of Natural Resources, 1594 West North Temple #3710, Box 145610, Salt Lake City, UT 84116-5610 or Equal Employment Opportunity Commission, 1801 L Street, NW, Washington DC 20507.*

---





# GEOLOGIC MAP OF THE PINTURA QUADRANGLE, WASHINGTON COUNTY, UTAH

by

*Hugh A. Hurlow and Robert F. Biek*

## ABSTRACT

This report describes selected aspects of the geology of the Pintura quadrangle. The quadrangle includes Permian through early Tertiary sedimentary rocks, middle Tertiary intrusive and volcanic rocks, and Quaternary volcanic rocks and surficial deposits. Mesozoic to early Cenozoic compressional deformation in the Utah-Idaho-Wyoming section of the Sevier orogenic belt, followed by Cenozoic magmatism and extensional faulting, created complex structural relations within the quadrangle. These structures are the main focus of this report.

Five major structures, including the Pintura anticline, parts of the Virgin and Kanarra anticlines, an intervening buried syncline, and the Hurricane fault, formed during Mesozoic to Cenozoic tectonism. In addition, large masses of mid-Tertiary-age quartz monzonite porphyry of the Pine Valley Mountains are at structurally and topographically low elevations in the quadrangle. This structural complexity, coupled with the fact that critical relationships are concealed by late Tertiary to Quaternary deposits in the hanging wall of the Hurricane fault, has led to conflicting structural interpretations of the area. The principal controversies concern the existence of the Pintura anticline and the timing and magnitude of displacement on the late Tertiary Hurricane fault. Stratigraphic units important to interpreting these structures include the late Campanian to early Paleocene Canaan Peak Formation, which unconformably overlies the Jurassic Navajo Sandstone in the suspected hinge zone of the Pintura anticline, and Quaternary basalt exposed on either side of the trace of the Hurricane fault.

Our mapping provides detailed field data and observations that help constrain and focus, but not necessarily resolve, these debates. We conclude that an important structural culmination occupies the suspected hinge zone of the Pintura anticline, but reinterpret this feature as a composite fold that formed first during late Mesozoic to early Cenozoic contractional deformation, then was modified during Tertiary time by extensional faulting and large-scale reverse drag in the hanging wall of the Hurricane fault.

## INTRODUCTION

The Pintura quadrangle is in Washington County, southwestern Utah, about 20 miles (32 km) northeast of St. George and 30 miles (48 km) southwest of Cedar City (figures 1 and 2). Although no large towns lie within the quadrangle, it is bisected by Interstate 15 and is affected by the 86 percent population increase experienced by Washington County between 1990 and 2000 (Utah Governor's Office of Planning and Budget, 2001). This population increase has resulted in dramatically greater demand for local natural resources, especially ground water, and the location of residential developments in areas of moderate to high geologic hazards. The climate in the Pintura quadrangle is semiarid; mean annual precipitation varies from less than 12 inches (30 cm) near Anderson Junction to about 20 inches (50 cm) in the eastern foothills of the Pine Valley Mountains (Cordova, 1978). Several perennial streams flow through the quadrangle, including Ash Creek, Wet Sandy, and Leeds Creek, whose sources are in the eastern Pine Valley Mountains, and LaVerkin Creek, whose source is east of the quadrangle (figure 3).

This pamphlet describes selected aspects of the geology of the Pintura quadrangle, including major structures; the field relations, ages, and geochemistry of Quaternary basalt; and some natural resources. Discussion of these and other aspects of the geology of the Pintura quadrangle and surrounding area - including stratigraphic units, geologic hazards, and geologic resources - can be found in Dobbin (1939), Gregory and Williams (1947), Cook (1957, 1960), Kurie (1966), Watson (1968), Rowley and others (1979), Stewart and others (1997), Hurlow (1998), Pearthree and others (1998), Lund and others (2001), and Biek (2003a, 2003b).

## TECTONIC SETTING

The Pintura quadrangle is in the transition zone between the Basin and Range and Colorado Plateau physiographic



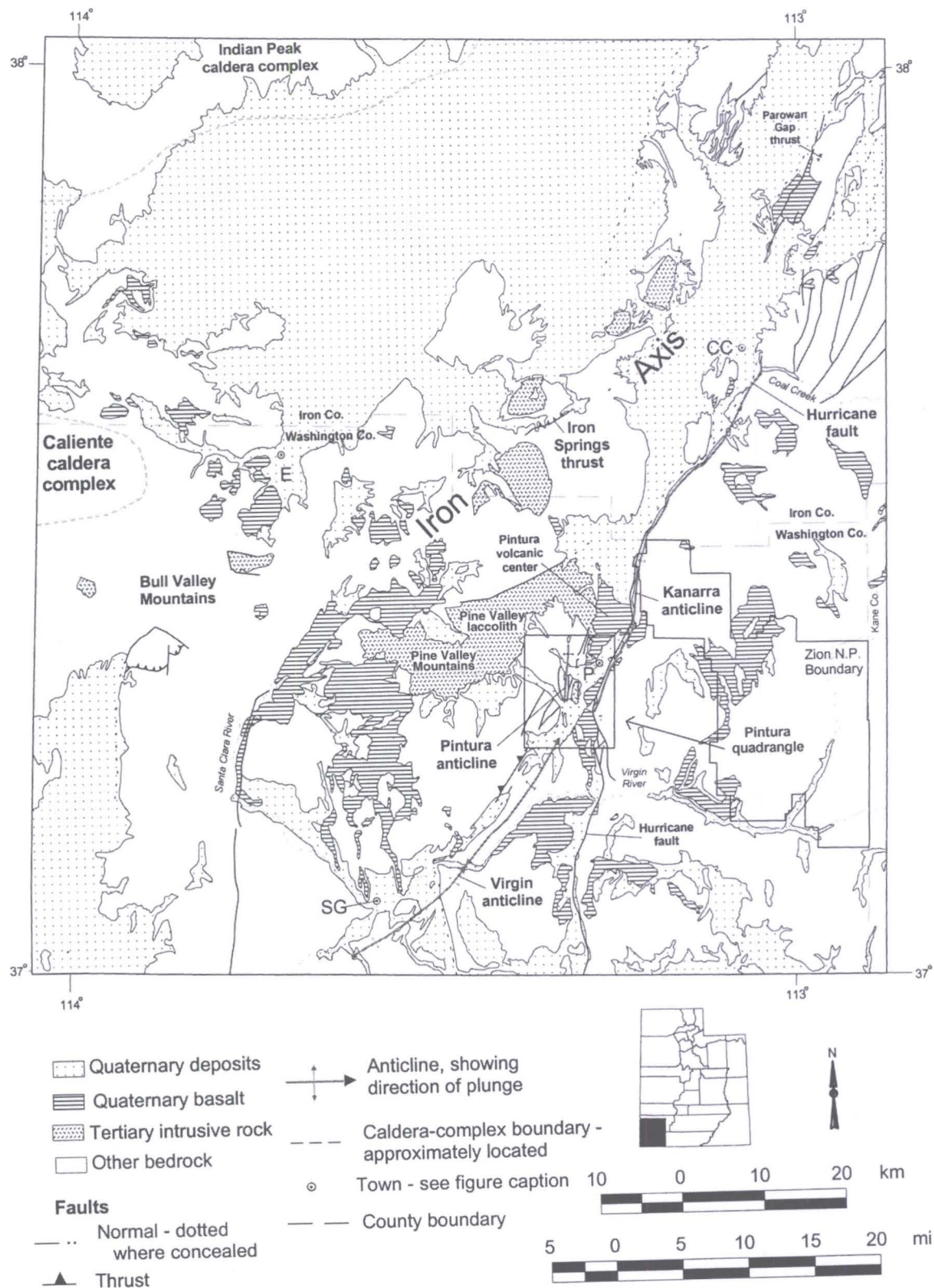
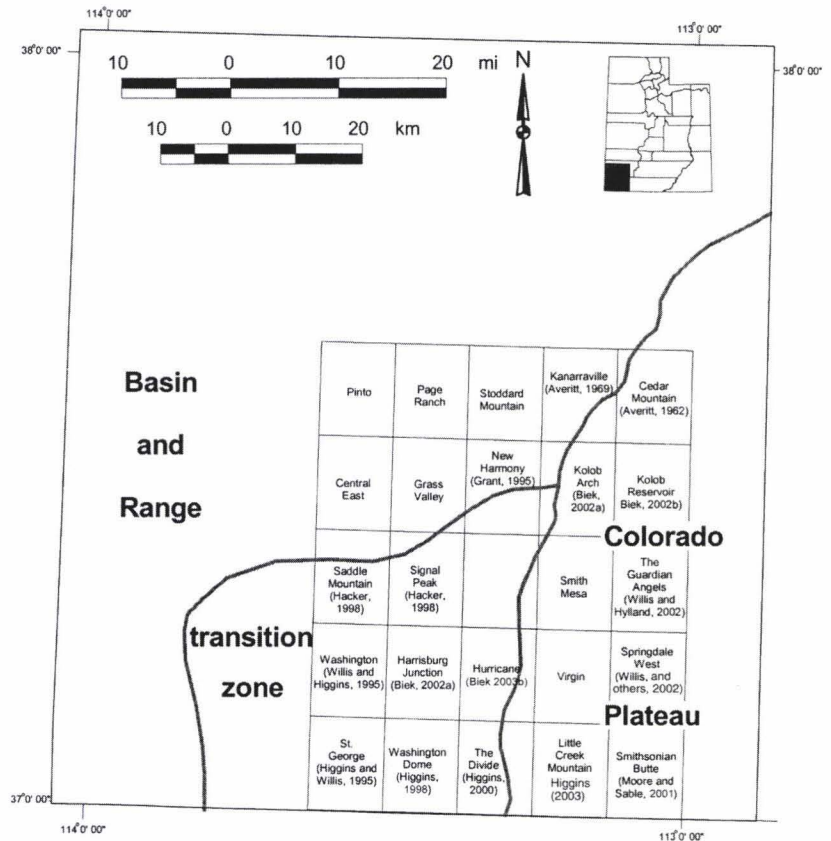


**Figure 1.** Generalized geologic map of southwestern Utah in the vicinity of the Pintura quadrangle, after Hintze and others (2000). Towns: CC = Cedar City; E = Enterprise; P = Pintura; and SG = St. George.



**Figure 2.** Locations of Basin and Range, Colorado Plateau, and transition zone physiographic provinces, and of the Pintura and surrounding quadrangles, in southwestern Utah. Published geologic maps shown with author reference.



provinces (figures 1 and 2) (Heylman, 1963; Best and Hamblin, 1978; Scott and Swadley, 1995; Maldonado and Nealey, 1997). The Basin and Range Province in southwest Utah is characterized by superposition of Cenozoic volcanism and normal faulting on Mesozoic to early Cenozoic contractional structures. The Mesozoic structures are part of the Utah-Idaho-Wyoming section of the Cordilleran fold and thrust belt, characterized by deformed Paleozoic and Mesozoic carbonate and siliciclastic strata (Armstrong, 1968; Royse and others, 1975; Allmendinger, 1992; Willis, 1999). The Colorado Plateau is underlain by strata deposited east of the Cordilleran hinge line, and is structurally simpler than the Basin and Range Province. The transition zone contains structural and stratigraphic characteristics of both provinces.

During the Sevier orogeny, uplift and erosion in eastern Nevada and western Utah associated with thrust faulting and folding led to fluvial deposition of the Iron Springs Formation in southwestern Utah during Late Cretaceous time (Fillmore, 1991; Goldstrand, 1994). Contractional deformation migrated eastward into southwestern Utah during latest Cretaceous to early Paleocene time, forming: (1) in the Pintura quadrangle, the Pintura and Kanarra anticlines, an intervening syncline (not exposed), and thrust faults that cut the east limb of the Kanarra anticline (cross section A-A') (Gregory and Williams, 1947; Cary, 1963; Kurie, 1966; Watson, 1968); (2) the Virgin anticline southwest of the Pintura quadrangle (figure 1) (Dobbin, 1939; Higgins and Willis, 1995; Biek, 2003a, 2003b; Higgins, 1998); and (3) several thrust faults and folds in the Cedar City area north and northeast of the quadrangle (figure 1) (Threet, 1963; van Kooten, 1988; Maldonado and Williams, 1993a). As explained below, the existence of the Pintura anticline and related syncline is contro-

versial. The timing of Late Cretaceous to early Cenozoic contractional deformation is constrained in part by strata exposed in the Pintura quadrangle. Fluvial strata of the late Campanian to early Paleocene Canaan Peak Formation record the waning stages of contractional deformation, whereas the Paleocene-Eocene Claron Formation was deposited after that deformation had ceased (Taylor, 1993; Goldstrand, 1994). In the Pintura quadrangle, the Canaan Peak Formation comprises fluvial conglomerate deposited on the suspected hinge zone of the Pintura anticline; this formation was only recently identified in the eastern Pine Valley Mountains (R.E. Anderson, written communication to P.M. Goldstrand in Goldstrand, 1992), and is more extensively exposed in south-central Utah (Bowers, 1972; Goldstrand, 1994).

During Oligocene to Quaternary time, volcanism and extension occurred throughout southwestern Utah. Oligocene to early Miocene calc-alkaline ash-flow tuff, volcanic mudflow breccia, and lava flows covered most of southwestern Utah; their source areas were primarily the Indian Peak and Caliente caldera complexes in western Utah and eastern Nevada, though local sources were also active in the Bull Valley Mountains about 25 miles (40 km) west-northwest of Pintura, and other local areas (figure 1) (Cook, 1960; Mackin, 1960; Rowley and others, 1979; Rowley and others, 1995; McKee and others, 1997). Relatively minor normal faulting and crustal extension accompanied the eruption of these volcanic rocks (Best and Christiansen, 1991; Rowley and others, 1995).

Quartz monzonite porphyry laccoliths of the "iron axis" were emplaced around 21 million years ago, including the Pine Valley laccolith, part of which crops out in the Pintura quadrangle (figure 1) (Cook, 1957, 1960; Blank and others,



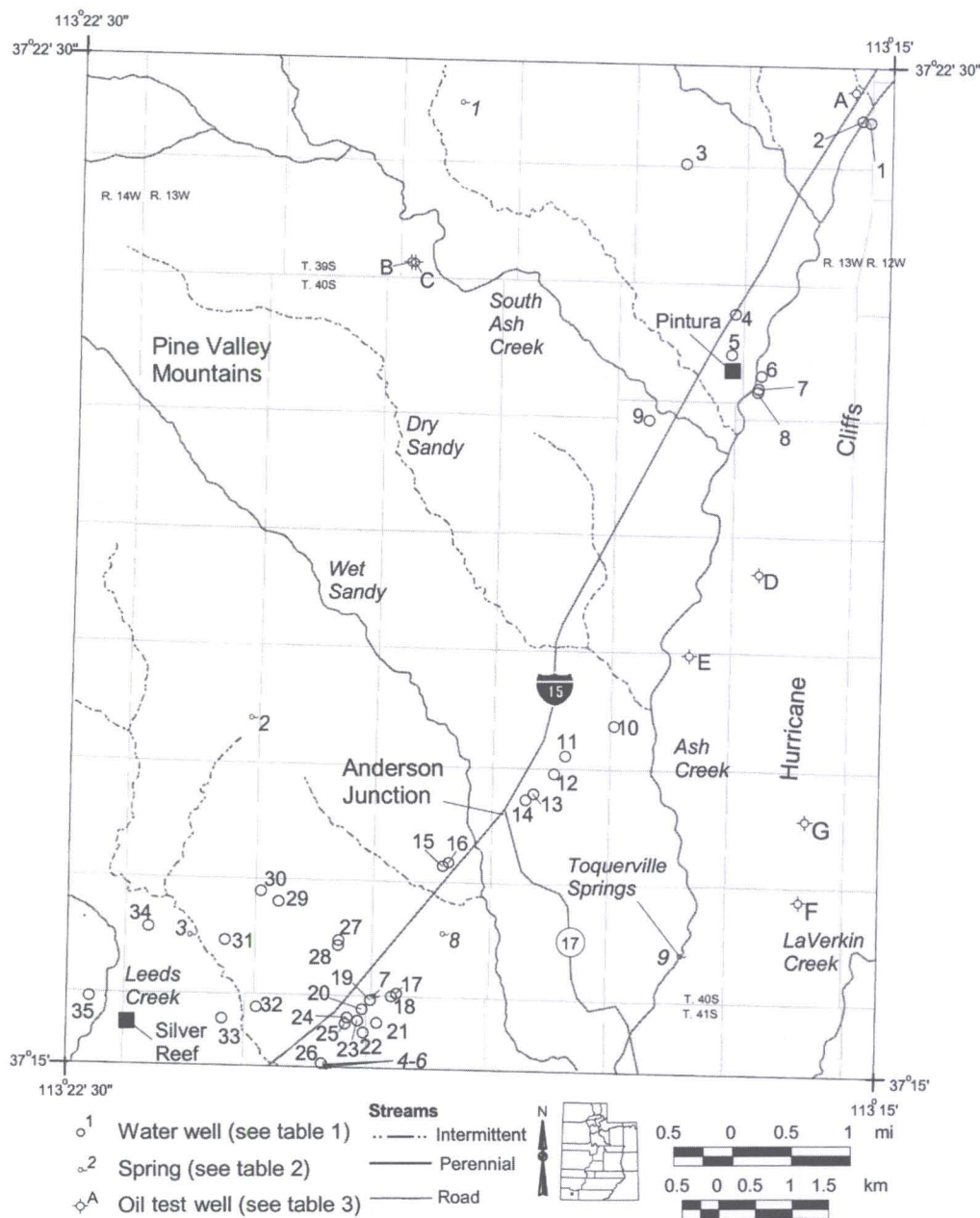


Figure 3. Geographic and hydrologic features of the Pintura quadrangle.

1992; McKee and others, 1997; Hacker, 1998). The Pine Valley laccolith chiefly intruded the middle part of the Claron Formation parallel to bedding (Cook, 1957, 1960; Hacker, 1998), but also locally intruded the lower part of the Iron Springs Formation in the Pintura quadrangle (see below). Intrusion of the Pine Valley laccolith rapidly uplifted the land surface, resulting in large landslides off the uplifted roof of the intrusion (Cook, 1957; Blank and others, 1992; Hacker, 1998; Hacker and others, 2002). These landslides consist of megabreccia deposits now exposed north and west of the Pine Valley Mountains (Cook, 1957; Blank and others, 1992; Hacker, 1998); such deposits presumably once covered much of the Pintura quadrangle, but have largely been removed by erosion or are now covered by younger deposits. A small erosional remnant of one of these megabreccia de-

posits is present in the northwestern part of section 2, T. 40 S., R. 13 W. in the Pintura quadrangle. Viscous, autobrecciated lava flows erupted from the areas evacuated by the landslides (Cook, 1957; Hacker, 1998); small outcrops of such flows are in the northern part of the Pintura quadrangle.

Basin and Range extension on steeply dipping normal faults accompanied by bimodal basaltic and rhyolitic volcanism began in southwestern Utah (at least north of the Pintura quadrangle) during late Miocene time, after emplacement of the iron-axis intrusions (Anderson and Mehnert, 1979). Two generations of normal faults formed in the Pintura quadrangle during Basin and Range extension, as described below; the older set is pre-Quaternary age, and the younger set includes the late Tertiary-Quaternary Hurricane fault and associated faults in its hanging wall.



## GEOLOGIC STRUCTURES IN THE PINTURA QUADRANGLE

The Pintura quadrangle contains five major structural features, including the Pintura anticline and parts of the Virgin and Kanarra anticlines and associated thrust faults, an intervening buried syncline, and the Hurricane fault. As discussed below, the existence of the Pintura anticline and the syncline between the Pintura and Kanarra anticlines is uncertain. In addition, large blocks of the quartz monzonite porphyry of the Pine Valley Mountains are present at a structurally and topographically low elevation compared to the main mass of the intrusion. Because some of this structure is "hidden" in the cross-bedded Navajo Sandstone, and because late Tertiary and Quaternary deposits in the hanging wall of the Hurricane fault conceal critical structures, interpretations of the area differ. Although much remains speculative, our new geologic mapping further constrains structural interpretations of this area.

### Pintura Anticline

The existence of the Pintura anticline has long been debated in the literature. Because the age of this structure provides important constraints on the timing of Sevier-age folding in southwestern Utah, a short review of previous work is in order. Huntington and Goldthwait (1904, 1905) and Gardner (1941, 1952) depicted the Pintura anticline in the north-central part of the Pintura quadrangle. Neighbor

(1952) briefly described the structure and a dry oil-exploration hole (Sun Oil Company No. 1 Pintura Unit; see table 3) drilled in the hinge zone of the Pintura anticline; he estimated the anticline had about 1,400 feet (430 m) of closure. Cook (1957) doubted the presence of the Pintura anticline, and correctly noted that its existence involves deciphering the attitude of the Navajo Sandstone, which is difficult to determine given its large-scale cross-beds. Cook noted that the easternmost outcrop of the Carmel-Navajo contact - in Leap Creek drainage in the adjacent New Harmony quadrangle (see also Grant, 1995) - dips northwest and is overlain in angular unconformity by the Claron Formation. He also noted that when the Claron is rotated back to horizontal, the Carmel-Navajo contact dips even more steeply northwest. Cook (1957) thus saw no evidence of a fold axis or east limb and therefore doubted the Pintura anticline is a Sevier-age fold. We agree with Cook's assessment that direct evidence of the Pintura anticline as a Sevier-age structure lies hidden in the great, sweeping cross-beds of Navajo Sandstone, and that when the Claron is rotated back to horizontal the Carmel everywhere dips to the northwest.

To more accurately map the axial plane of the fold, Cary (1963) used a color break in the Navajo Sandstone as a proxy for a paleohorizontal surface by contouring the interval between the color break and the base of the Carmel (figure 4). He determined that the Pintura anticline was doubly plunging with about 2,000 feet (600 m) of closure on the Navajo Sandstone, but did not take a position as to the origin of the fold.

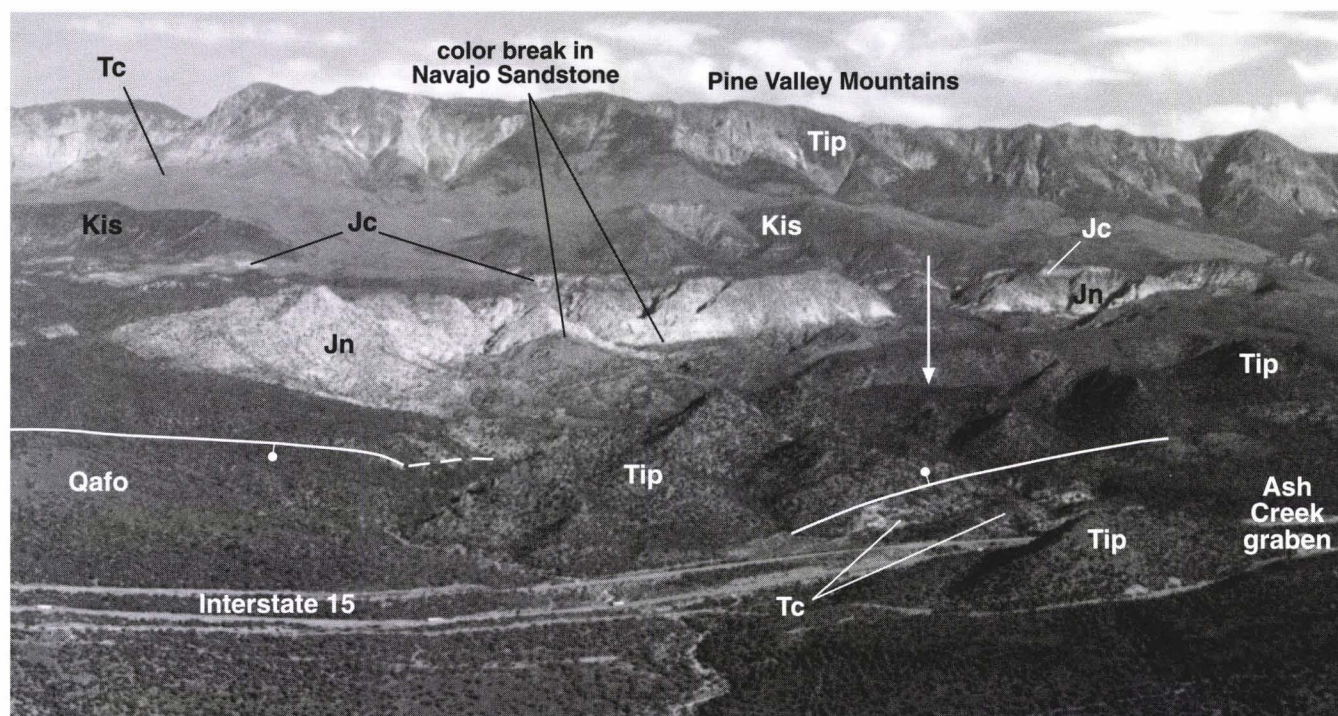


**Figure 4.** View to the northwest of the west-central part of the Pintura quadrangle from southern Black Ridge. The quartz monzonite porphyry of the Pine Valley Mountains (unit Tip) west of Interstate 15 is about 3,000 feet below the main mass of the laccolith (visible in the background), and may be a satellitic intrusion or an erosional remnant of a once-continuous sheet. The structurally low position of this quartz monzonite porphyry is due to the combined effects of (1) normal faults bounding either side of the body (shown by solid lines where visible; the trace of the western fault is concealed behind the main body; the arrow shows its position), and (2) reverse drag in the hanging wall of the Hurricane fault and/or other west-side-down normal faults. The base of the quartz monzonite porphyry here is discordant with bedding in the underlying Claron Formation, indicating faulting during or prior to intrusion. Qafo = early Quaternary alluvial-fan deposits; Tip = quartz monzonite porphyry of the Pine Valley Mountains; Tc = Claron Formation (Oligocene-Eocene); Kis = Iron Springs Formation (Cretaceous); Jc = Carmel Formation (Jurassic); Jn = Navajo Sandstone (Jurassic).



Our mapping reveals the following evidence regarding the controversy over the Pintura anticline.

1. In the north-central Pintura quadrangle, the Claron Formation depositionally overlies the Navajo Sandstone and Canaan Peak Formations in sections 27, 28, 33, and 34, T. 39 S., R. 13 W., but overlies the Carmel Formation both northeast and west of this area. The Claron Formation was, therefore, deposited above an angular unconformity developed on an erosionally beveled structural culmination. Where the Canaan Peak and Claron Formations unconformably overlie the Navajo Sandstone, erosion has removed more than 4,000 feet (1,220 m) of stratigraphic section, including all of the Upper Cretaceous Iron Springs Formation. This unconformity establishes the age of the structural culmination as between early and late Campanian time (about 84 to 72 Ma), the youngest known age of the Iron Springs Formation and the oldest known age of the Canaan Peak Formation, respectively (Goldstrand, 1992, 1994), but both dates are poorly constrained and are derived from outside the quadrangle. This culmination most likely formed either in the hinge zone of an anticline or along the trace of a reverse fault, and continued at least 5 miles (8 km) south to section 28, T. 40 S., R. 13 W., the southernmost exposure of the Canaan Peak Formation.
2. The Carmel Formation presently shows a reversal in dip direction in the north-central part of the Pintura quadrangle (plate 1) and the southern part of the New Harmony quadrangle (Grant, 1995). In the Pintura quadrangle the western limb, hinge zone, and eastern limb of the Pintura anticline are exposed in three distinct outcrop areas. In the western exposure area, in the NW<sup>1</sup>/<sub>4</sub> of section 28 and the NE<sup>1</sup>/<sub>4</sub> and south-central parts of section 29, T. 39 S., R. 13 W., the Carmel dips about 14 to 34 degrees west to west-northwest. In the central exposure area, in the N<sup>1</sup>/<sub>4</sub> of section 28, T. 39 S., R. 13 W., the Carmel dips 10 to 35 degrees north-northwest to north-northeast, with considerable local variation in attitude. We interpret these exposures as the broad hinge zone of the Pintura anticline; this hinge zone contains several open parasitic folds but generally dips gently to the north. In the eastern outcrop area, in the NW<sup>1</sup>/<sub>4</sub> of section 27, T. 39 S., R. 13 W., the Carmel dips about 10 to 12 degrees east to east-southeast, with local variations in attitude not shown on plate 1. High-angle normal faults cut both Jurassic and Tertiary units, accounting for some of the local structural variation in all three outcrop areas. As noted above, when the Claron Formation is rotated to horizontal, bedding in the exposed Carmel Formation everywhere restores to westward dips. If a pre-Hurricane fault Pintura anticline existed, its hinge is concealed beneath younger deposits east

of present exposures of Mesozoic rocks.

3. The Claron Formation dips 15 to 30 degrees east and is cut by numerous normal faults, complicating the restoration of the Pintura anticline's early Tertiary configuration.

Considering the evidence listed above, we are left with two plausible interpretations for the original configuration of the Pintura anticline during latest Cretaceous to early Tertiary time. (1) The Pintura anticline was actually a west-facing homocline formed above a thrust-fault ramp or splay. This thrust fault flattened east of the homocline, then ramped upward again to form the Kanarra anticline. (2) The Pintura anticline was a broad anticline whose east limb formed the west limb of a syncline that separates the Pintura and Kanarra anticlines. We favor the second interpretation, mainly on the presence of the Late Cretaceous to early Paleocene structural culmination described above and lack of evidence of an associated reverse fault. Cross section A-A' (plate 2) reflects this interpretation; in that section, the dip of the east limb of the Pintura anticline is poorly constrained and was modified from its original configuration by an unknown amount of reverse drag in the hanging wall of the Hurricane fault.

On the map we place the axial trace of the Pintura anticline along the present dip reversal in the Carmel Formation in the north-central part of the Pintura quadrangle, and continue it south along the outcrop belt of Canaan Peak Formation, recognizing that these features occupy a broad, poorly defined, composite hinge zone. Our axial trace is about 0.5 to 1 mile (0.8-1.6 km) east of that shown by Cary (1963). This hinge zone formed as a late Mesozoic-early Cenozoic contractional fold, and then was modified in the axis of a large-scale reverse-drag fold in the hanging wall of the Hurricane fault. This large-scale reverse drag is to us the most likely explanation for the eastward tilting of the Claron Formation.

### Kanarra Anticline

The Kanarra anticline strikes northeast parallel to the Hurricane Cliffs in the east-central part of the Pintura quadrangle where it folds exposed Permian and Triassic units; the fold continues 30 miles (48 km) north to Cedar City (figure 1) (Gregory and Williams, 1947; Threet, 1963; Kurie, 1966; Averitt and Threet, 1973). Grant and others (1994) depicted the Kanarra anticline as a fault-propagation fold, related to an east-directed thrust fault in the subsurface.

The Hurricane fault truncates the Kanarra anticline just northeast of Anderson Junction (figure 5). The east limb and part of the crest of the fold are well exposed in the Hurricane Cliffs and in the LaVerkin Creek drainage. Near the top of the cliffs, Fossil Mountain strata generally dip 20 to 30 degrees east. Dips increase considerably down the east limb of the fold and beds are locally overturned. Only part of the west limb of the Kanarra anticline is preserved in the foot-wall of the Hurricane fault; near the fault, normal fault drag accentuates dips on the west limb. The axial plane of the Kanarra anticline probably dips steeply west.

The west-directed Taylor Creek thrust fault cuts the east limb of the Kanarra anticline and, in its best exposures at the



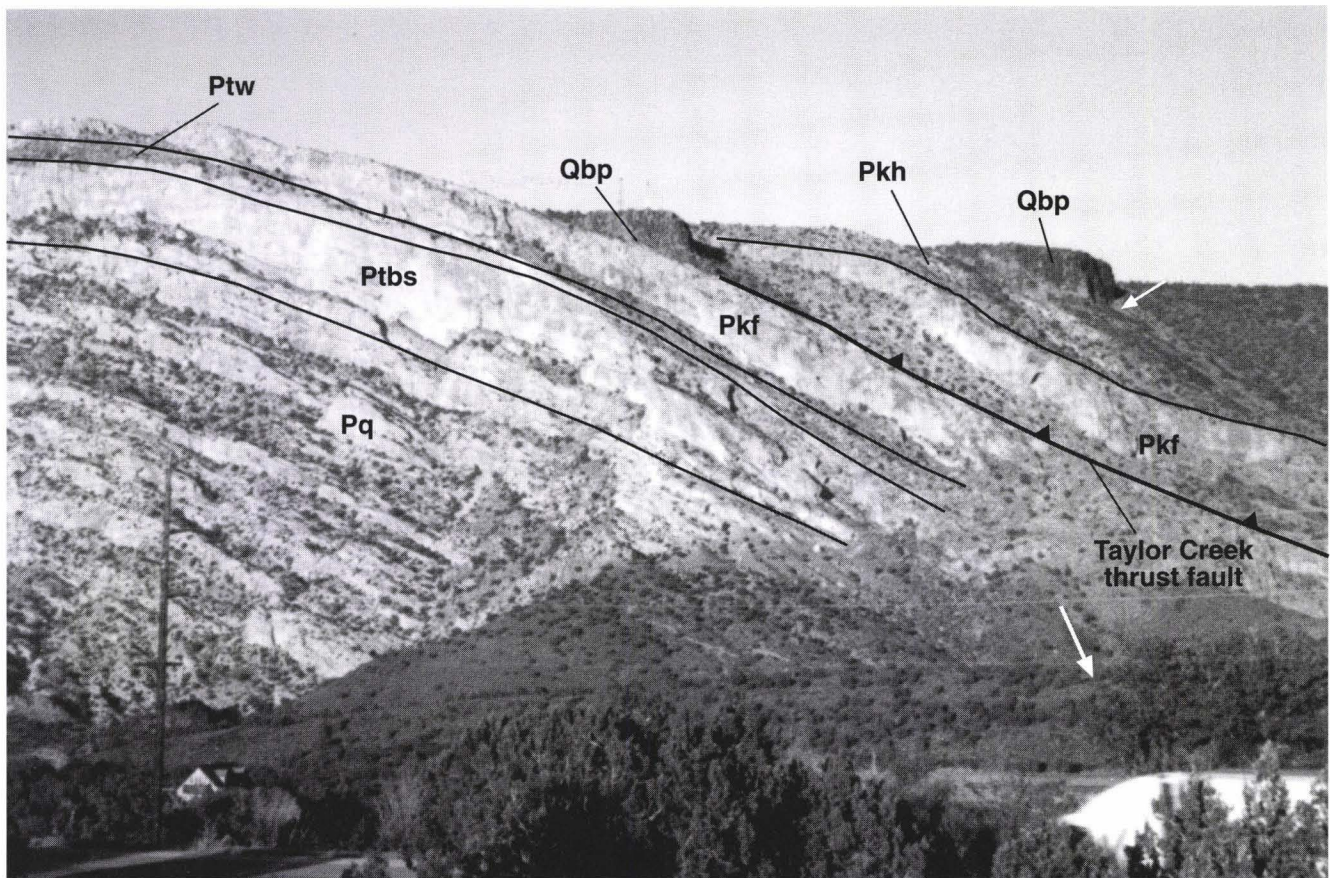


**Figure 5.** View to the east of the Hurricane Cliffs at the southern edge of Black Ridge, sections 23, 24, 25, 26, T. 40 S., R. 13 W. The trace of the Hurricane fault is along the slope break at the base of the cliffs. The cliffs are composed of Permian strata of the Queantoweap Sandstone (Pq), the Brady-Seligman (Ptbs) and Woods Ranch (Ptw) Members of the Toroweap Formation, and the Fossil Mountain (Pkf) and Harrisburg (Pkh) Members of the Kaibab Formation. Beds dip about 20 to 35 degrees southeast on the east limb of the Kanarra anticline. The Fossil Mountain Member is repeated by the west-directed Taylor Creek thrust fault. Quaternary basalt of the Pintura flow (Qbp) overlies the Permian strata on the southern margin of the cliffs, and is also exposed at the base of the cliffs. Stewart and Taylor (1996) correlated basalt outcrops on the hanging wall and footwall of the Hurricane fault based on geochemistry (white arrows show approximate locations of the samples), indicating about 1,480 feet (450 m) of stratigraphic separation across the fault since the basalt erupted about 880,000 years ago.

south end of Black Ridge, places the Lower Permian Fossil Mountain Member of the Kaibab Formation over the Lower Triassic lower red member of the Moenkopi Formation (figure 6). In the hanging wall of the Taylor Creek thrust fault in the eastern half of section 13, T. 40 S., R. 13 W., the lower Moenkopi and Kaibab Formations are overturned, and the middle red member of the Moenkopi Formation is tightly folded into northeast-trending anticlines and synclines. Several smaller east- and west-directed thrust faults displace the Virgin Limestone and middle red members of the Moenkopi Formation in the hanging wall of the Taylor Creek thrust fault. We interpret this overturning and small-scale folding as the result of deformation in the footwall of a small, east-directed thrust fault (cross section A-A').

### Older Tertiary Normal Faults

Older normal faults generally strike north to northeast, have relatively short traces, and include both southeast- and northwest-side-down displacement senses. The older normal faults cut pre-Quaternary units but are concealed by Quaternary surficial deposits. Most of the older faults are likely

younger than about 21 million years, the age of the quartz monzonite porphyry of the Pine Valley Mountains, but some may be older (see following discussion in "Interpretation of the Quartz Monzonite Porphyry of the Pine Valley Mountains"). Older-generation faults in the east-central part of the quadrangle that cut the Jurassic Carmel Formation and Navajo Sandstone form a complex array, and the displacement on some of these faults may have included transcurrent and/or scissors-like motion. North-northeast-striking normal faults in the north-central part of the quadrangle include both west- and east-side-down displacement senses, and continue northward into the New Harmony quadrangle (Grant, 1995).

The largest and tectonically most important of the older normal faults is in the south-central part of the quadrangle, about 1 to 2 miles (1.5-3 km) northwest of Interstate 15, along the southeastern margin of the foothills of the Pine Valley Mountains (figure 4). This down-to-the-east fault is mostly concealed; it may comprise a single, continuous trace with subsidiary splays, or a fault zone consisting of several en echelon and roughly co-linear faults. On the map the fault is illustrated as a single trace and is dotted where concealed.

This fault or fault zone strikes north in its northernmost extent, and gradually curves to an east-northeast strike in its



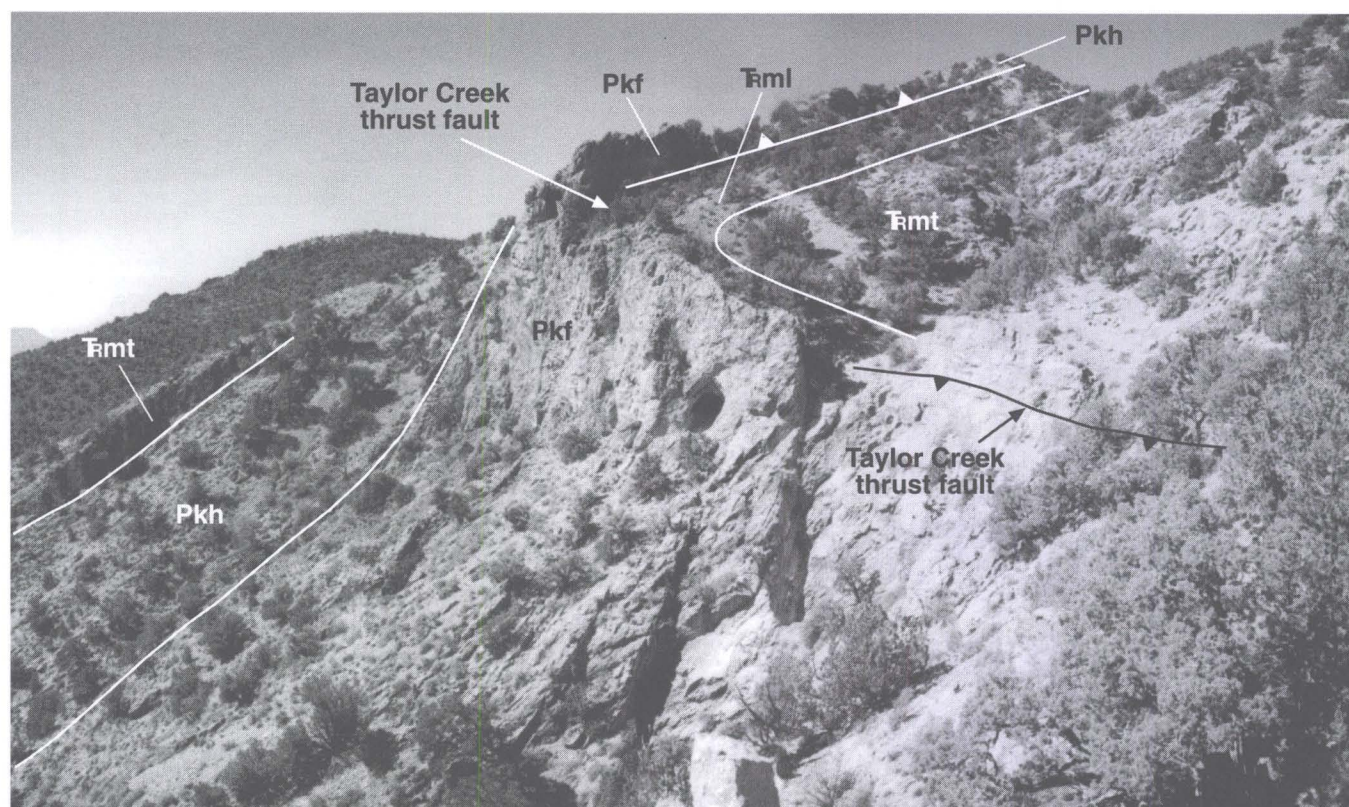


**Figure 6.** View southwest to the Taylor Creek thrust fault in the SW $\frac{1}{4}$  section 24, T. 40 S., R. 13 W. The thrust here is folded and dips very steeply east and southeast; it is partly hidden from view by the Fossil Mountain cliffs. It places steeply east-southeast-dipping Kaibab strata (Fossil Mountain [Pkh] and Harrisburg [Pkh] Members) over the lower red (Tml) and Timpoweap (Tmt) Members of the Moenkopi Formation.

southwesternmost exposure; its trace length is about 6 miles (10 km). The northern part of the fault (in section 9, T. 40 S., R. 13 W.) juxtaposes a hanging wall composed of the upper part of the Navajo Sandstone, the overlying Canaan Peak and Claron Formations, and quartz monzonite porphyry of the Pine Valley Mountains against a footwall composed of the lower part of the Navajo Sandstone; this represents a stratigraphic separation of about 500 to 1,500 feet (150–460 m). A southern splay of this part of the fault displaces map unit Qafo (pre-Holocene) by approximately 100 to 150 feet (30–45 m), indicating continued motion or reactivation during Pleistocene time (figure 4). A small exposure at about 4,120 feet (1,255 m) elevation in an unnamed wash in section 21, T. 40 S., R. 13 W., juxtaposes a hanging wall of Claron Formation overlying the Canaan Peak Formation with a footwall of Navajo Sandstone. Stratigraphic displacement on this fault is difficult to determine given complex faulting of Navajo, Temple Cap, and Carmel strata 1 to 2 miles (1.5–3 km) to the west, absence of these beds east of the fault, and pre-Canaan Peak paleotopography developed on the Navajo Sandstone. Displacement is probably between a few hundred feet and 1,500 feet (up to 460 m).

This fault and another, subparallel but down-to-the-west fault about one mile (1.5 km) to the east together form a graben that bounds a large block of quartz monzonite porphyry of the Pine Valley Mountains in the center of the quadrangle, in the W $\frac{1}{2}$  sections 10 and 15, T. 40 S., R. 13 W. (figure 4). The eastern fault is exposed in an excavation (labeled a prospect near the center of section 15) where it places the quartz monzonite porphyry down on the west against the

lower Claron Formation; farther north, the fault places the Claron Formation against the Navajo Sandstone.

Another fault is exposed in a gully east of the latter fault described in the preceding paragraph and immediately west of Interstate 15, in the west-central part of section 15, T. 40 S., R. 13 W. (plate 1). This east-side-down fault juxtaposes a hanging wall of quartz monzonite porphyry of the Pine Valley Mountains against a footwall of upper Claron Formation. Whereas the previously described faults have brittle deformation fabrics where exposed, the “gully fault” is a 3- to 4-foot-thick (1–3 m) mylonitic zone developed in the Claron Formation. The gully fault likely formed relatively shortly after intrusion of the quartz monzonite porphyry of the Pine Valley Mountains, accounting for the mylonitic crystal-plastic deformation fabrics. The extent and tectonic significance of the gully fault are uncertain.

### Hurricane Fault

The Hurricane fault is a late Tertiary-Quaternary, west-side-down normal fault that strikes north to northeast and extends for about 160 miles (250 km) from the Grand Canyon, Arizona, to Cedar City, Utah (figure 1) (Huntington and Goldthwait, 1904; Dobbin, 1939; Gardner, 1941; Hamblin, 1965; Kurie, 1966; Anderson and Mehnert, 1979; Hamblin and others, 1981; Anderson and Christenson, 1989; Stewart and Taylor, 1996; Pearthree and others, 1998; Lund and others, 2001). The Hurricane fault lies near the base of the rugged Hurricane Cliffs. The Hurricane fault consists of



relatively straight sections separated by relatively sharp bends (Stewart and Taylor, 1996; Stewart and others, 1997; Lund and Everitt, 1998; Higgins, 2000; Biek, 2003b). The straight sections were referred to as geometric segments by Stewart and Taylor (1996) and as sections by Pearthree and others (1998); Lund and others (2001) presented evidence that suggests that at least some of these segments/sections are true seismogenic segments. These geometric segments/sections are about 6 to 25 miles (10-40 km) long and consist of closely spaced, steeply dipping, sub-parallel normal faults. The bends, referred to as geometric-segment boundaries by Stewart and Taylor (1996) and section boundaries by Pearthree and others (1998), consist of broad, structurally complex zones of faulting and folding (Stewart and Taylor, 1996; Stewart and others, 1997). The Pintura quadrangle contains the southern part of the Ash Creek geometric segment of the Hurricane fault and part of its southern geometric-segment boundary (Stewart and Taylor, 1996; Lund and Everitt, 1998; Lund and others, 2001; Biek, 2003b).

Estimates of the timing and amount of displacement on the Hurricane fault differ, although it is generally accepted that stratigraphic separation increases from south to north (Gardner, 1941; Kurie, 1966; Anderson and Mehnert, 1979; Stewart and others, 1997). Most workers think that motion on the Hurricane fault began no earlier than early Miocene time, and Anderson and Mehnert (1979) suggested that motion did not begin until Pliocene or Pleistocene time.

Attempts to estimate tectonic throw on the Hurricane fault are greatly complicated by deformation near the fault trace, and because the fault cuts and modifies the hinge zone and west limb of the Kanarra anticline (Hamblin, 1965; Kurie, 1966; Anderson and Mehnert, 1979; Anderson and Christenson, 1989). In the Pintura quadrangle, Stewart and Taylor (1996) measured about 1,480 feet (450 m) of stratigraphic separation of geochemically correlated Quaternary basalt exposed in the hanging wall and footwall (figure 5). For pre-Tertiary rocks, Stewart and Taylor (1996) estimated about 8,250 feet (2,520 m) of stratigraphic separation and Hurlow (1998) illustrated about 2,800 to 5,000 feet (850-1,500 m) of stratigraphic separation on the southern part of the Ash Creek segment of the Hurricane fault. Based on our new mapping, projection of the footwall geology to the Hurricane fault above the present land surface on cross section A-A' indicates throw of about 10,000 feet (3,000 m) on the base of the Navajo Sandstone, due to the combined effects of displacement on the Hurricane fault and reverse drag and normal faulting in its hanging wall. This estimate depends strongly on assumptions about the geometry of eroded parts of the Kanarra anticline, the subsurface shape of the Hurricane fault, and the subsurface geometry of the hanging wall.

Deformation of the hanging wall of the Hurricane fault in the Pintura quadrangle is extensive. Quaternary basalt exhibits reverse drag along the length of the fault, as demonstrated by map relations and by paleomagnetic data discussed below. The basalt is thus folded into an asymmetric anticline whose ill-defined axis parallels the Hurricane fault. This reverse drag flexure is cut by numerous normal faults. Anderson and Christenson (1989) and Lund and Everitt (1998) documented several east-side-down fault scarps in Quaternary basalt and Pleistocene alluvial fans between the Hurricane fault and the eastern Pine Valley Mountains, and named this region the Ash Creek graben (figure 4). Stewart

and Taylor (1996) described a small reverse fault and anticline in Quaternary basalt within the segment boundary in the southern part of the Pintura quadrangle. As noted above, we interpret the east dip of the Claron Formation as evidence for large-scale reverse drag in the hanging wall of the Hurricane fault. Reverse drag forms in response to curvature of the fault plane, and the greater magnitude and extent of this folding in the Claron Formation than in the basalt is due to protracted, pre-Quaternary motion on the Hurricane fault.

### Interpretation of the Quartz Monzonite Porphyry of the Pine Valley Mountains

Several masses of quartz monzonite porphyry of the Pine Valley Mountains lie 0.5 to 3 miles (0.8-5 km) west of Interstate 15 in the Pintura quadrangle. These outcrops are enigmatic because: (1) their basal contacts are about 3,000 feet (900 m) lower than the basal contact of the main body of the Pine Valley laccolith, (2) their basal contacts are structurally discordant with bedding in underlying sedimentary rocks, and (3) one of these masses locally overlies the lower part of the Iron Springs Formation. In contrast, the main mass of the Pine Valley laccolith, exposed about 5 miles (8 km) to the west in the Pine Valley Mountains, consistently intrudes the middle part of the Claron Formation parallel to bedding, which dips gently toward the center of the laccolith everywhere the intrusive contact is exposed (Cook, 1957, 1960; Hacker, 1998).

Three plausible interpretations explain these anomalous masses of the Pine Valley laccolith: (1) they are gravity-slide blocks, (2) they represent local, satellitic intrusions of the Pine Valley laccolith, or (3) they are erosional remnants of the once-continuous laccolith, which originally extended at least as far east as the present location of Interstate 15. We do not believe that these masses are gravity-slide blocks, due to the absence of brecciation of the quartz monzonite porphyry along its basal contact except near known faults, and because subjacent sedimentary rocks locally display low-grade contact metamorphism similar to that observed along the base of the main laccolith body. Interpretations (2) and (3) seem equally plausible. Anderson and Mehnert (1979) first reported, and coauthor Biek mapped, deeply weathered blocks of quartz monzonite porphyry of the Pine Valley Mountains caught in the Hurricane fault near the Kolob Canyons (Biek, 2002a). Whether these blocks, and those in the Pintura quadrangle, were once part of a much larger laccolith, or are satellite intrusions, is unknown.

We interpret the angular discordance between the intrusion base and bedding in the underlying Claron Formation, and the local intrusion into the Iron Springs Formation, to reflect pre-intrusion faulting and related tilting. The best candidates for pre-quartz monzonite porphyry faults are in the west-central part of the quadrangle (see discussion of "Older Tertiary Normal Faults" above); one of these faults cuts the Claron, Iron Springs, and Carmel Formations but is truncated by the quartz monzonite porphyry, in section 18, T. 40 S., R. 13 W. There, the Claron Formation dips about 20 to 30 degrees northeast below the subhorizontal intrusive contact. The base of the large mass of quartz monzonite porphyry just west of Interstate 15 in the central part of the quadrangle dips gently southeast to south and is discordant



with bedding in the underlying Claron Formation, which dips about 20 to 40 degrees east to southeast (section 15, T. 40 S., R. 13 W.). A pre-intrusion, west-side-down normal fault may be responsible for the dip of the Claron Formation and the repetition of section on either side of the quartz monzonite body; this fault was either covered (laccolith interpretation) or intruded (satellitic intrusion interpretation) by the quartz monzonite porphyry.

If the masses of quartz monzonite porphyry of the Pine Valley Mountains are indeed in place, they owe their low structural position to the combined effects of post-intrusion faulting and large-scale reverse drag in the hanging wall of the Hurricane fault. Another possibility, difficult to prove, is that these masses intruded at lower structural levels than the main laccolith. As noted above, the largest mass occupies a graben between two older normal faults; the western fault accommodated about 500 feet (150 m) of throw.

### Discussion of Cross Section

Cross section A-A' illustrates many aspects of the structure of the Pintura quadrangle described above, including the Kanarra and Pintura anticlines and a postulated intervening buried syncline, the Taylor Creek thrust and related faults, and the Hurricane fault with associated faulting and reverse drag in its hanging wall. Several features in cross section A-A' are poorly constrained. The curved geometry of the Hurricane fault is based on requirements of reverse drag as shown in cross sections drawn by Hamblin (1965). The dip of the fault near the surface is based on a single fault-plane exposure immediately southeast of Pintura, and by numerous exposures in the Hurricane quadrangle to the south, all of which indicate the fault dips 65 to 75 degrees near the surface (Biek, 2003b). The geometry of the eastern limb of the Pintura anticline and of the adjacent syncline are largely unknown, because no outcrops or subsurface data are available to constrain their location, shape, or magnitude.

All folds in cross section A-A' were constructed using the kink-band method (Suppe and Medwedeff, 1990), maintaining constant stratal thickness. The dip of Tertiary rocks in the hanging wall of the Hurricane fault is based on down-dip projection of the Claron Formation, which dips about 30 degrees east in its easternmost exposures. This approach creates up to about 2,800 vertical feet (850 m) of "space" between the top of the Claron Formation and the base of Quaternary basalt in the subsurface. We therefore assume that quartz monzonite porphyry of the Pine Valley Mountains, associated megabreccia deposits, and late Tertiary clastic deposits overlie the Claron Formation in the subsurface along the line of section. Several water-well logs (table 1 and figure 3) provide minimum estimates of the subsurface thickness of unconsolidated deposits and Quaternary basalt in the hanging wall of the Hurricane fault.

### QUATERNARY BASALT

Quaternary basalt exposed on the hanging wall and foot-wall of the Hurricane fault in southwestern Utah and northwestern Arizona is useful in analyzing the displacement history and style of the Hurricane fault and the geomorphic evo-

**Table 1.** Water wells in the Pintura quadrangle<sup>1</sup>.

ID <sup>2</sup>	Point of diversion <sup>3</sup>	Sec <sup>3</sup>	T <sup>3</sup>	R <sup>3</sup>
1	S 590 W 129 E4	25	39 S	13 W
2	S 500 W 500 E4	25	39 S	13 W
3	N 130 W 450 S4	26	39 S	13 W
4	S 1290 W 420 NE	2	40 S	13 W
5	S 510 W 550 E4	2	40 S	13 W
6	S 1553 E 800 W4	1	40 S	13 W
7	S 1680 E 836 W4	1	40 S	13 W
8	S 1824 E 800 W4	1	40 S	13 W
9	N 5160 E 1390 SW	11	40 S	13 W
10	N 1948 E 135 SW	23	40 S	13 W
11	N 575 E 620 S4	22	40 S	13 W
12	S 235 E 135 N4	27	40 S	13 W
13	S 1135 W 825 N4	27	40 S	13 W
14	S 138 W 1188 N4	27	40 S	13 W
15	N 795 E 425 S4	28	40 S	13 W
16	N 428 E 540 S4	28	40 S	13 W
17	N 172 E 1137 SW	33	40 S	13 W
18	S 44 E 1151 NW	4	41 S	13 W
19	S 203 E 193 NW	4	41 S	13 W
20	S 605 W 183 NE	5	41 S	13 W
21	S 1180 E 505 NW	4	41 S	13 W
22	S 1650 W 125 NE	5	41S	13 W
23	S 1131 W 375 N	5	41 S	13 W
24	S 1059 E 1863 N4	5	41 S	13 W
25	S 1345 E 1776 N4	5	41 S	13 W
26	S 3111 E 699 N4	5	41 S	13 W
27	N 2513 W 1444 SE	32	40 S	13 W
28	N 2308 W 1526 SE	32	40 S	13 W
29	S 1000 E 1100 NW	32	40 S	13 W
30	S 541 E 217 NW	32	40 S	13 W
31	S 136 W 1364 E4	31	40 S	13 W
32	S 618 E 486 NW	5	41 S	13 W
33	S 1133 W 1062 NW	5	41 S	13 W
34	N 2958 E 1124 SW	31	40 S	13 W
35	S 132 W 1554 NE	1	41 S	14 W

#### Notes:

1. Data from Utah Division of Water Rights (<http://waterrights.utah.gov>).
2. Corresponds to number on figure 3.
3. Location is given in "Point of Diversion" (POD) notation.  
NW, NE, SW, and SE refer to the northwest, northeast, southwest and southeast section corners, respectively.  
N4, S4, E4, and W4 = midpoint of northern, southern, eastern, and western section boundary lines, respectively.  
Sec = Section, T = Township, R = Range.  
Example: well 1 is located 590 feet south and 129 feet west of the midpoint of the east boundary line of section 25 in T. 39 S., R. 13 W., relative to the Salt Lake Base Line and Meridian.



lution of the region (Hamblin, 1963, 1965; Anderson and Mehnert, 1979; Hamblin and others, 1981; Anderson and Christenson, 1989; Stewart and Taylor, 1996; Pearthree and others, 1998; Willis and others, 1999; Lund and others, 2001; Willis and Biek, in press). Lund and others (2001) used geochemical, geochronologic, and paleomagnetic investigations of Quaternary basalt adjacent to the Hurricane fault to calculate long-term slip rates, which we briefly summarize here.

Minor and trace element geochemistry shows that the basaltic flows in the Pintura quadrangle consist of three distinct geochemical groups, each of which is widely distributed and present on both sides of the Hurricane fault. These flows are part of the Pintura volcanic field, whose eruptive center is just west of Interstate 15 and just north of the Pintura quadrangle (Grant, 1995; Lund and Everitt, 1998). Smaller vents are known atop Black Ridge at "Mystery Hill" in the Smith Mesa quadrangle, (Ben Everitt, Utah Division of Water Resources, written communication, 2000) and co-author Biek mapped cinder deposits near Ash Creek Reservoir dam in the Kolob Arch quadrangle (Biek, 2002a). The Pintura flows yielded  $^{40}\text{Ar}/^{39}\text{Ar}$  plateau ages of  $0.84 \pm 0.03$  Ma and  $0.81 \pm 0.10$  Ma from samples within the quadrangle (appendix; Lund and others, 2001). Samples of Pintura flow rocks from outside of the Pintura quadrangle yielded  $^{40}\text{Ar}/^{39}\text{Ar}$  plateau ages of  $0.89 \pm 0.02$  Ma,  $0.88 \pm 0.05$  Ma, and  $0.87 \pm 0.04$  Ma (Lund and others, 2001; Biek, 2003b).

Paleomagnetic data indicate that basalt in the hanging wall of the Hurricane fault, in sections 14, 23, and 26 of T. 40 S., R. 13 W., has been tilted about 10 to 25 degrees toward the fault (M. Hozik in Lund and Everitt, 1998). These results agree with the conclusions of Hamblin (1965) that reverse

drag, related to the curvature of the Hurricane fault, is an important aspect of deformation of its hanging wall and complicates estimates of tectonic throw on the fault. Using geochemically correlated, dated basalt flows, and accounting for the effects of hanging-wall deformation, Lund and others (2001) determined a long-term slip rate for the Hurricane fault at the south end of Black Ridge of 0.018 inches/year (0.45 mm/yr); farther north, near Exit 36 on Interstate 15, they calculated a long-term slip rate of 0.023 inches/year (0.57 mm/yr).

## ECONOMIC RESOURCES

Water is perhaps the most important and valuable resource in the Pintura quadrangle, considering the rapid population growth and arid climate of Washington County. Wells and springs in the quadrangle are shown on figure 3 and are listed in tables 1 and 2. Toquerville Springs provide culinary water to several public-supply entities. A well drilled by Washington County Water Conservancy District southwest of Anderson Junction in section 28, T. 40 S., R. 13 W. (well 15, table 1) produces water from the Navajo Sandstone. An aquifer test conducted by the U.S. Geological Survey yielded transmissivity estimates of 18,000 square feet per day (1,670 m<sup>2</sup>/d) and 900 square feet per day (85 m<sup>2</sup>/d) from two observation wells, each about 380 feet (115 m) deep, but in different directions, from the pumping well (Heilweil and others, 2000). Their results indicate strongly anisotropic hydraulic conductivity in the Navajo Sandstone, resulting from a dense array of joints and faults that cut the

**Table 2.** Springs in the Pintura quadrangle<sup>1</sup>.

ID <sup>2</sup>	Name	CFS <sup>3</sup>	Point of Diversion <sup>4</sup>	Sec <sup>4</sup>	T <sup>4</sup>	R <sup>4</sup>
1	Deer Spring	0.013	N 4000 E 2400 SW	28	39 S	13 W
2	Blue Spring	0.015	N 2000 W 300 SE	19	40 S	13 W
3.	Unnamed Spring	0.018	N 2600 W 2900 SE	31	40 S	13 W
4.	Unnamed Spring	0.089	S 3070 W 1833 NE	5	41 S	13 W
5.	Unnamed Spring	0.089	S 3145 W 1790 NE	5	41 S	13 W
6.	Unnamed Spring	0.089	S 3210 W 1783 NE	5	41 S	13 W
7.	Danish Ranch Domestic Spring/Stream	1.5	S 20 E 340 NW	4	41 S	13 W
8.	Danish Ranch Domestic Spring/Stream	1.5	N 345 W 2120 E4	33	40 S	13 W
9.	Toquerville Springs	1.97	N 2125 E 735 S4	35	40 S	13 W

**Notes:**

1. Data from Utah Division of Water Rights (<http://nrwt1.nr.state.ut.us>).

2. Corresponds to number on figure 3.

3. Water right in cubic feet per second.

4. Location is given in "Point of Diversion" (POD) notation.

NW, NE, SW, and SE refer to the northwest, northeast, southwest and southeast section corners, respectively.

N4, S4, E4, and W4 = midpoint of northern, southern, eastern, and western section boundary lines, respectively.

Sec = Section, T = Township, R = Range.

Example: spring 1 is located 4,000 feet north and 2,400 feet east of the southwest corner of section 28 in T. 39 S., R. 13 W., relative to the Salt Lake Base Line and Meridian.



**Table 3.** *Petroleum-test wells in the Pintura quadrangle<sup>1</sup>.*

ID <sup>2</sup>	Operator	Well Name	Spot <sup>3</sup>	Sec <sup>3</sup>	T <sup>3</sup>	R <sup>3</sup>	API Number <sup>4</sup>	Year	Elevation (feet)	Total Depth (feet)	Formation Tops <sup>5</sup>
A	Neptune Explor. Co.	1-25 FEDERAL	2060 FNL 721 FEL	25	39 S	13 W	4305330024	1976	4250	2610	Log not available
B	Pan American Co.	1 PINTURA UNIT	675 FSL 505 FWL	33	39 S	13 W	4305310879	1962	5272	9501	Tcp 915; Tcs 2635; Tmu 2800; Pkh 4585; Pqu 5390; Pp 6730; Mc 7470; Mr 8140; Du 8925
C	Sun Oil Co.	1 UNIT	398 FSL 872 FWL	33	39 S	13 W	4305311164	1951	5250	5496	Tcp 905; Tcs 2550; Tmu 2727; Pkh 4998
D	Pease Oil & Gas Co.	1-13 FEDERAL	1625 FNL 1140 FWL	13	40 S	13 W	4305330007	1972	4351	3171	Mr 1466; Du 3995
E	McCulloch Oil Co.	1 GOVT-WOLF	90 FNL 3515 FWL	23	40 S	13 W	4305310704	1964	3799	7315	Fault 375; Mr 792; Du 1742; Fault 3375; TD in Cambrian strata
F	Titan Oil Co.	36-C1 STATE	660 FNL 1980 FEL	36	40 S	13 W	4305330003	1969	4200	4124	Pq 1620; Pp 3180; Mc 3784
G	Buttes Oil & Gas Co.	Pease Federal #1	3050 FSL 1725 FEL	25	40 S	13 W	4305320318	1967	4340	5236	Log not available

**Notes:**<sup>1</sup> Data from U.S. Bureau of Reclamation.<sup>2</sup> Corresponds to letter on figure 3.<sup>3</sup> Location is given as distance in feet from section lines. FNL = from north line, FSL = from south line, FEL = from east line, FWL = from west line, Sec = Section, T = Township, R = Range, relative to Sale Lake Base Line and Meridian.<sup>4</sup> American Petroleum Institute Petroleum information (PI) database number.<sup>5</sup> Data from UGS unpublished records. Formation tops are in feet. Unit abbreviations are same as on map and in Explanation of Map Units.

unit (Cordova, 1978; Hurlow, 1998; Heilweil and others, 2000). Fractures are abundant in the Navajo Sandstone throughout the Pintura quadrangle, and likely formed during both Cretaceous and Tertiary-Quaternary deformation.

Several oil-test wells in the Pintura quadrangle tested Paleozoic and Mesozoic units along anticlinal folds (figure 3; table 3); none produced significant shows of oil or natural gas. Numerous gravel pits are in alluvial fans derived from the Pine Valley Mountains and Hurricane Cliffs. The Navajo Sandstone was quarried for local use as dimension stone in section 28, T. 40 S., R. 13 W., near Anderson Junction. The old town site and part of the White Reef portion of the Silver Reef mining district are in the southwest corner of the quadrangle. Biek (2003a, 2003b) reviewed the geology and history of the Silver Reef mining district. He also provided a more complete treatment of the geologic resources and geologic hazards of the Hurricane quadrangle to the south - much of that discussion is relevant to the Pintura quadrangle.

## ACKNOWLEDGMENTS

This project was jointly funded by the Utah Geological Survey (UGS) and U.S. Geological Survey (USGS) under STATEMAP agreement No. 99HQAG0138. Hurlow mapped areas west of Interstate 15 and Utah Highway 17; Biek mapped areas to the east. Ernie Anderson (USGS) graciously shared his knowledge of the area, and spent a day in the field discussing structurally complex parts of the quadrangle. We also thank Bill Lund (UGS) and Ben Everitt (Utah Division of Water Resources) for sharing their knowledge of the Hurricane fault and Pintura basalt flow. We appreciate the very thorough reviews of Ernie Anderson (USGS), Pete Rowley (USGS), Doug Sprinkel (UGS), and Mike Hylland (UGS); Sandy Eldredge, Bill Lund, Bryce Tripp, and Janae Wallace, each with the UGS, also reviewed portions of the report.



## REFERENCES

- Allmendinger, R.W., 1992, Fold and thrust tectonics of the western United States exclusive of the accreted terranes, *in* Burchfiel, B.C., Lipman, P.W., and Zoback, M.L., editors, *The Cordilleran orogen - conterminous U.S.*: Boulder, Colorado, Geological Society of America, *The Geology of North America*, v. G-3, p. 583-607.
- Anderson, R.E., and Christenson, G.E., 1989, Quaternary faults, folds, and selected volcanic features in the Cedar City 1° x 2° quadrangle, Utah: Utah Geological and Mineralogical Survey Miscellaneous Publication 89-6, 29 p., 1 plate, scale 1:250,000.
- Anderson, R.E., and Mehnert, H.H., 1979, Reinterpretation of the history of the Hurricane fault in Utah, *in* Newman, G.W., and Goode, H.D., editors, 1979 Basin and Range Symposium: Rocky Mountain Association of Geologists and Utah Geological Association, p. 145-165.
- Armstrong, R.L., 1968, Sevier orogenic belt in Nevada and Utah: Geological Society of America Bulletin, v. 79, p. 429-458.
- 1970, Geochronology of Tertiary igneous rocks, eastern Great Basin and Range Province, western Utah, eastern Nevada, and vicinity, U.S.A.: *Geochimica et Cosmochimica Acta*, v. 34, p. 203-232.
- Averitt, Paul, 1962, Geology and coal resources of the Cedar Mountain quadrangle, Iron County, Utah: U.S. Geological Survey Professional Paper 389, 71 p., 3 plates, scale 1:24,000.
- 1969, Geology of the Kanarrville quadrangle, Iron County, Utah: U.S. Geological Survey Geologic Quadrangle Map GQ-694, 1 plate, scale 1:24,000.
- Averitt, Paul, and Threet, R.L., 1973, Geologic map of the Cedar City quadrangle, Iron County, Utah: U.S. Geological Survey Geologic Quadrangle Map GQ-1120, scale 1:24,000.
- Best, M.G., and Christiansen, E.H., 1991, Limited extension during peak Tertiary volcanism, Great Basin of Nevada and Utah: *Journal of Geophysical Research*, v. 96, p. 13,509-13,528.
- Best, M.G., and Hamblin, W.K., 1978, Origin of the northern Basin and Range Province - implications from the geology of its eastern boundary: Geological Society of America Memoir 152, p. 313-340.
- Best, M.G., Scott, R.B., Rowley, P.D., Swadley, W.C., Anderson, R.E., Gromme, C.S., Harding, A.E., Deino, A.L., Christiansen, E.H., Tingey, D.G., and Sullivan, K.R., 1993, Oligocene-Miocene caldera complexes, ash-flow sheets, and tectonism in the central and southeastern Great Basin, *in* Lahren, M.M., Trexler, J.H., Jr., and Spinosa, Claude, editors, *Crustal evolution of the Great Basin and Sierra Nevada: Field trip guide*, Geological Society of America, Cordilleran and Rocky Mountain Sections Meeting, p. 285-311.
- Biek, R.F., 2002a, Interim geologic map of the Kolob Arch quadrangle, Washington and Iron Counties, Utah: Utah Geological Survey Open-File Report 386, 33 p., scale 1:24,000.
- 2002b, Interim geologic map of the Kolob Reservoir quadrangle, Washington and Iron Counties, Utah: Utah Geological Survey Open-File Report 376, 22 p., scale 1:24,000.
- 2003a, Geologic map of the Harrisburg Junction quadrangle, Washington County, Utah: Utah Geological Survey Map 191, 42 p., 2 plates, scale 1:24,000.
- 2003b, Geologic map of the Hurricane quadrangle, Washington County, Utah: Utah Geological Survey Map 187, 61 p., 2 plates, scale 1:24,000.
- Blakey, R.C., 1994, Paleogeographic and tectonic controls on some Lower and Middle Jurassic erg deposits, Colorado Plateau, *in* Caputo, M.V., Peterson, J.A., and Franczyk, K.J., editors, *Mesozoic systems of the Rocky Mountain region, USA*: Denver, Colorado, Rocky Mountain Section of the Society for Sedimentary Geology, p. 273-298.
- Blank, H.R., Rowley, P.D., and Hacker, D.B., 1992, Miocene monzonitic intrusions and associated megabreccia of the iron axis region, southwestern Utah: Utah Geological Survey Miscellaneous Publication 92-3, p. 399-420.
- Bowers, W.E., 1972, The Canaan Peak, Pine Hollow, and Wasatch Formations in the Table Cliff region, Garfield County, Utah: U.S. Geological Survey Bulletin 1331-B, 39 p.
- Cary, R.S., 1963, Pintura anticline, Washington County, Utah, *in* Heylman, E.B., editor, *Geology of the southwestern transition between the Basin-Range and Colorado Plateau, Utah*: Salt Lake City, Intermountain Association of Petroleum Geologists 12th Annual Field Conference, Guidebook to the Geology of Southwestern Utah, p. 172-179.
- Clemmensen, L.B., Olsen, Henrik, and Blakey, R.C., 1989, Erg-margin deposits in the Lower Jurassic Moenave Formation and Wingate Sandstone, southern Utah: Geological Society of America Bulletin, v. 101, p. 759-773.
- Cook, E.F., 1957, Geology of the Pine Valley Mountains, Utah: Utah Geological and Mineralogical Survey Bulletin 58, 111 p.
- 1960, Geologic atlas of Utah, Washington County: Utah Geological and Mineralogical Survey Bulletin 70, 119 p., scale 1:125,000.
- Cordova, R.M., 1978, Ground-water conditions in the Navajo Sandstone in the central Virgin River basin, Utah: Utah Department of Natural Resources Technical Publication 61, 66 p.
- DeCourten, Frank, 1998, *Dinosaurs of Utah*: Salt Lake City, University of Utah Press, 300 p.
- Deino, Alan, and Potts, Robert, 1990, Single-crystal  $^{40}\text{Ar}/^{39}\text{Ar}$  dating of the Olorgesailie Formation, southern Kenya rift: *Journal of Geophysical Research*, v. 95, p. 8453-8470.
- Dobbin, C.E., 1939, Geologic structure of St. George District, Washington County, Utah: American Association of Petroleum Geologists Bulletin, v. 23, p. 121-144.
- Dubiel, R.F., 1994, Triassic deposystems, paleogeography, and paleoclimate of the Western Interior, *in* Caputo, M.V., Peterson, J.A., and Franczyk, K.J., editors, *Mesozoic systems of the Rocky Mountain region, USA*: Rocky Mountain Section of Society of Economic Paleontologists and Mineralogists, p. 133-168.
- Fillmore, R.P., 1991, Tectonic influence on sedimentation in the southern Sevier foreland, Iron Springs Formation (Upper Cretaceous), southwestern Utah, *in* Nations, J.D., and Eaton, J. G., editors, *Stratigraphy, depositional environments, and sedimentary tectonics of the western margin, Cretaceous Western Interior seaway*: Geological Society of America Special Paper 260, p. 9-25.
- Fleck, R.J., Sutter, J.F., and Elliot, D.H., 1977, Interpretation of discordant  $^{40}\text{Ar}/^{39}\text{Ar}$  age spectra of Mesozoic tholeiites from Antarctica: *Geochimica et Cosmochimica Acta*, v. 41, p. 15-32.
- Gardner, L.S., 1941, The Hurricane fault in southwestern Utah



- and northwestern Arizona: *American Journal of Science*, v. 239, p. 241-260.
- 1952, The Hurricane fault, in Thune, H.W., editor, Guidebook to the geology of Utah No. 7 – Cedar City, Utah to Las Vegas, Nevada: Intermountain Association of Petroleum Geologists, p. 15-21.
- Goldstrand, P.M., 1992, Evolution of Late Cretaceous and early Tertiary basins of southwest Utah based on clastic petrology: *Journal of Sedimentary Petrology*, v. 62, no. 3, p. 495-507.
- 1994, Tectonic development of Upper Cretaceous to Eocene strata of southwestern Utah: *Geological Society of America Bulletin*, v. 106, p. 145-154.
- Grant, S.K., 1995, Geologic map of the New Harmony quadrangle, Washington County, Utah: Utah Geological Survey Miscellaneous Publication 95-2, 14 p., 2 plates, scale 1:24,000.
- Grant, S.K., Fielding, L.W., and Noweir, M.A., 1994, Cenozoic fault patterns in southwestern Utah and their relationships to structures of the Sevier orogeny, in Blackett, R.E., and Moore, J.N., editors, Cenozoic geology and geothermal systems of southwestern Utah: Utah Geological Association Publication 23, p. 39-153.
- Gregory, H.E., and Williams, N.C., 1947, Zion National Monument: *Geological Society of America Bulletin*, v. 58, p. 211-244.
- Hacker, D.B., 1998, Catastrophic gravity sliding and volcanism associated with the growth of laccoliths - examples from early Miocene hypabyssal intrusions of the Iron Axis magmatic province, Pine Valley Mountains, southwestern Utah: Kent, Ohio, Kent State University, Ph.D. dissertation, 258 p., 5 plates.
- Hacker, D.B., Holm, D.K., Rowley, P.D., and Blank, H.R., 2002, Associated Miocene laccoliths, gravity slides, and volcanic rocks, Pine Valley Mountains and Iron Axis region, southwestern Utah, in Lund, W.R., editor, Field guide to geologic excursions in southwestern Utah and adjacent areas of Arizona and Nevada: U.S. Geological Survey Open-File Report OF 02-0172, p. 235-283.
- Hamblin, W.K., 1963, Late Cenozoic basalts of the St. George basin, Utah, in Heylman, E.B., editor, Guidebook to the geology of southwestern Utah -- Transition between the Basin-Range and Colorado Plateau provinces: Salt Lake City, Intermountain Association of Petroleum Geologists 12th Annual Field Conference, p. 84-89.
- 1965, Origin of "reverse drag" on the downthrown side of normal faults: *Geological Society of America Bulletin*, v. 76, p. 1,145-1,164.
- Hamblin, W.K., Damon, P.E., and Bull, W.B., 1981, Estimates of vertical crustal strain rates along the western margins of the Colorado Plateau: *Geology*, v. 9, p. 293-298.
- Heilweil, V.M., Freethy, G.W., Stolp, B.J., Wilkowske, C.D., and Wilberg, D.E., 2000, Geohydrology and numerical simulation of ground-water flow in the central Virgin River basin of Iron and Washington Counties, Utah: Utah Department of Natural Resources Technical Publication 116, 139 p.
- Hesse, C.J., 1935, *Semionotus cf. gigas* from the Triassic of Zion Park: *American Journal of Science*, 5th series, v. 29, p. 526-531.
- Heylman, E.B., editor, 1963, Guidebook to the geology of southwestern Utah – Transition between the Basin-Range and Colorado Plateau provinces: Salt Lake City, Intermountain Association of Petroleum Geologists 12th Annual Field Conference, 232 p.
- Hayden, J.M., 2003, Interim geologic map of the Little Creek Mountain quadrangle, Washington County, Utah: Utah Geological Survey Open-File Report 417, scale 1:24,000.
- Higgins, J.M., 1998, Interim geologic map of the Washington Dome quadrangle, Washington County, Utah: Utah Geological Survey Open-File Report 363, 128 p., 2 plates, scale 1:24,000.
- 2000, Interim geologic map of The Divide quadrangle, Washington County, Utah: Utah Geological Survey Open-File Report 378, 61 p., 2 plates, scale 1:24,000.
- Higgins, J.M., and Willis, G.C., 1995, Interim geologic map of the St. George quadrangle, Washington County, Utah: Utah Geological Survey Open-File Report 323, 108 p., 2 plates, scale 1:24,000.
- Hintze, L.F., Willis, G.C., Laes, D.Y.M., Sprinkel, D.A., and Brown, K.D., 2000, Digital geologic map of Utah: Utah Geological Survey Map 179DM, CD, scale 1:500,000.
- Huntington, Ellsworth, and Goldthwait, J.W., 1904, The Hurricane fault in the Toquerville district, Utah: *Harvard Museum Camp Zoology Bulletin*, v. 42, p. 199-259.
- 1905, The Hurricane fault in southwestern Utah: *Journal of Geology*, v. 11, p. 45-63.
- Hurlow, H.A., 1998, The geology of the central Virgin River basin, southwestern Utah, and its relation to ground-water conditions: Utah Geological Survey Water Resource Bulletin 26, 53 p., 6 plates.
- Imlay, R.W., 1980, Jurassic paleobiogeography of the conterminous United States in its continental setting: U.S. Geological Survey Professional Paper 1062, 134 p.
- Kurie, A.E., 1966, Recurrent structural disturbance of Colorado Plateau margin near Zion National Park, Utah: *Geological Society of America Bulletin*, v. 77, p. 867-872.
- Lambert, R.E., 1984, Shnabkaib Member of the Moenkopi Formation - depositional environment and stratigraphy near Virgin, Washington County, Utah: Brigham Young University Geology Studies, v. 31, pt. 1, p. 47-65.
- Lund, W.R., and Everitt, B.J., 1998, Reconnaissance paleoseismic investigation of the Hurricane fault in southwestern Utah, in Pearthree, P.A., Lund, W.R., Stenner, H.D., and Everitt, B.L., Paleoseismologic investigations of the Hurricane fault in southwestern Utah and northwestern Arizona - final project report: National Earthquake Hazards Reduction Program, External Research, Chapter 2, p. 8-48.
- Lund, W.R., Pearthree, P.A., Amoroso, Lee, Hozik, M.J., and Hatfield, S.C., 2001, Paleoseismic investigation of earthquake hazard and long-term movement history of the Hurricane fault, southwestern Utah and northwestern Arizona - final technical report: National Earthquake Hazards Reduction Program, External Research, Program Element I, Panel NI, Award No. 99HQGR0026, 120 p.
- Mackin, J.H., 1960, Structural significance of Tertiary volcanic rocks in southwestern Utah: *American Journal of Science*, v. 258, p. 81-131.
- Maldonado, Florian, and Nealey, L.D., editors, 1997, Geologic studies in the Basin and Range-Colorado Plateau transition zone in southeastern Nevada, southwestern Utah, and northwestern Arizona, 1995: U.S. Geological Survey Bulletin 2153, 288 p.
- Maldonado, Florian, and Williams, V.S., 1993a, Geologic map of the Paragonah quadrangle, Iron County, Utah: U.S. Geological Survey Geologic Quadrangle Map GQ-1713, scale 1:24,000.
- 1993b, Geologic map of the Parowan Gap quadrangle, Iron



- County, Utah: U.S. Geological Survey Geologic Quadrangle Map GQ-1712, scale 1:24,000.
- McKee, E.D., 1938, The environment and history of the Toroweap and Kaibab Formations of northern Arizona and southern Utah: Carnegie Institute of Washington Publication 492, 268 p.
- McKee, E.H., Blank, H.R., and Rowley, P.D., 1997, Potassium-argon ages of Tertiary igneous rocks in the eastern Bull Valley Mountains and Pine Valley Mountains, southwestern Utah, in Maldonado, Florian, and Nealey, L.D., editors, Geologic studies in the Basin and Range-Colorado Plateau transition zone in southeastern Nevada, southwestern Utah, and northwestern Arizona, 1995: U.S. Geological Survey Bulletin 2153, p. 243-252.
- Moore, D.W., and Sable, E.G., 2001, Geologic map of the Smithsonian Butte quadrangle, Washington County, Utah: Utah Geological Survey Miscellaneous Publication 01-1, 30 p., 2 plates, scale 1:24,000.
- Mullett, D.J., 1989, Interpreting the early Tertiary Claron Formation of southern Utah [abs.]: Geological Society of America Abstracts with Programs, v. 21, no. 5, p. 120.
- Mullett, D.J., Wells, N.A., and Anderson, J.J., 1988a, Early Cenozoic deposition in the Cedar-Bryce depocenter - certainties, uncertainties, and comparisons with other Flagstaff-Green River basins [abs.]: Geological Society of America Abstracts with Programs, v. 20, no. 3, p. 217.
- 1988b, Unusually intense pedogenic modification of the Paleocene-Eocene Claron Formation of southwestern Utah [abs.]: Geological Society of America Abstracts with Programs, v. 20, no. 5, p. 382.
- Neighbor, F., 1952, Geology of the Pintura structure, Washington County, Utah, in Thune, H.W., editor, Guidebook to the geology of Utah, No. 7: Intermountain Association of Petroleum Geologists, p. 79-80.
- Nielson, R.L., 1981, Depositional environment of the Toroweap and Kaibab Formations of southwestern Utah: Salt Lake City, University of Utah, Ph.D. dissertation, 495 p.
- 1986, The Toroweap and Kaibab Formations, southwestern Utah, in Griffen, D.T., and Phillips, W.R., editors, Thrusting and extensional structures and mineralization in the Beaver Dam Mountains, southwestern Utah: Utah Geological Association Publication 15, p. 37-53.
- 1991, Petrology, sedimentology and stratigraphic implications of the Rock Canyon Conglomerate, southwestern Utah: Utah Geological Survey Miscellaneous Publication 91-7, 65 p.
- Nielson, R.L., and Johnson, J.L., 1979, The Timpoweap Member of the Moenkopi Formation, Timpoweap Canyon, Utah: Utah Geology, v. 6, no. 1, p. 17-27.
- Pearthree, P.A., Lund, W.R., Stenner, H.D., and Everitt, B.L., 1998, Paleoseismologic investigations of the Hurricane fault in southwestern Utah and northwestern Arizona - final project report: National Earthquake Hazards Reduction Program, External Research, 125 p.
- Peterson, Fred, 1994, Sand dunes, sabkhas, streams, and shallow seas - Jurassic paleogeography in the southern part of the Western Interior basin, in Caputo, M.V., Peterson, J.A., and Franczyk, K.J., editors, Mesozoic systems of the Rocky Mountain region, USA: Denver, Colorado, Rocky Mountain Section of the Society for Sedimentary Geology, p. 233-272.
- Rawson, R.R., and Turner-Peterson, C.E., 1979, Marine-carbonate, sabkha, and eolian facies transitions within the Permian Toroweap Formation, northern Arizona, in Baars, D.L., editor, Permianland: Four Corners Geological Society Guidebook, 9th Field Conference, p. 87-99.
- Rowley, P.D., Nealey, L.D., Unruh, D.M., Snee, L.W., Mehnert, H.H., Anderson, R.E., and Gromme, C.S., 1995, Stratigraphy of Miocene ash-flow tuffs in and near the Caliente caldera complex, southeastern Nevada and southwestern Utah, in Scott, R.B., and Swadley, W.C., editors, Geologic studies in the Basin and Range-Colorado Plateau transition zone in southeastern Nevada, southwestern Utah, and northwestern Arizona, 1992: U.S. Geological Survey Bulletin 2056, p. 47-88.
- Rowley, P.D., Steven, T.A., Anderson, J.J., and Cunningham, C.G., 1979, Cenozoic stratigraphic and structural framework of southwestern Utah: U.S. Geological Survey Professional Paper 1149, 22 p.
- Royse, Frank, Jr., Warner, M.A., and Reese, D.L., 1975, Thrust belt structural geometry and related stratigraphic problems, Wyoming-Idaho-northern Utah, in Bolyard, D.W., editor, Deep drilling frontiers of the central Rocky Mountains: Rocky Mountain Association of Geologists, p. 41-54.
- Sable, E.G., and Maldonado, Florian, 1997, The Brian Head Formation (revised) and selected Tertiary sedimentary rock units, Markagunt Plateau and adjacent areas, southwestern Utah, in Maldonado, Florian, and Nealey, L.D., editors, Geologic studies in the Basin and Range-Colorado Plateau transition zone in southeastern Nevada, southwestern Utah, and northwestern Arizona, 1995: U.S. Geological Survey Bulletin 2153, p. 7-26.
- Samson, S.D., and Alexander, E.C., Jr., 1987, Calibration of the interlaboratory  $^{40}\text{Ar}/^{39}\text{Ar}$  dating standard, Mmhb-1: Chemical Geology and Isotopic Geoscience, v. 66, p. 27-34.
- Sansom, P.J., 1992, Sedimentology of the Navajo Sandstone, southern Utah, USA: Oxford, England, Wolfson College, Ph.D. dissertation, 291 p.
- Schaeffer, B., and Dunkle, D.H., 1950, A semionotid fish from the Chinle Formation, with consideration of its relationships: American Museum Novitates, no. 1457, p. 1-29.
- Scott, R.B., and Swadley, W.C., editors, 1995, Geologic studies in the Basin and Range-Colorado Plateau transition zone in southeastern Nevada, southwestern Utah, and northwestern Arizona, 1992: U.S. Geological Survey Bulletin 2056, 275 p.
- Sorauf, J.E., and Billingsley, G.H., 1991, Members of the Toroweap and Kaibab Formations, Lower Permian, northern Arizona and southwestern Utah: The Mountain Geologist, v. 28, no. 1, p. 9-24.
- Steiger, R.H., and Jäger, Eustace, 1977, Subcommittee on geochronology - Convention on the use of decay constants in geo- and cosmochronology: Earth and Planetary Science Letters, v. 36, p. 359-362.
- Stewart, J.H., Poole, F.G., and Wilson, R.F., 1972, Stratigraphy and origin of the Triassic Moenkopi Formation and related strata in the Colorado Plateau region, with a section on sedimentary petrology by R.A. Cadigan: U.S. Geological Survey Professional Paper 691, 195 p., scale 1:2,500,000.
- Stewart, M.E., and Taylor, W.J., 1996, Structural analysis and fault segment boundary identification along the Hurricane fault in southwestern Utah: Journal of Structural Geology, v. 18, p. 1,017-1,029.
- Stewart, M.E., Taylor, W.J., Pearthree, P.A., Solomon, B.J., and Hurlow, H.A., 1997, Neotectonics, fault segmentation and seismic hazards along the Hurricane fault in Utah and Arizona - an overview of environmental factors in an actively extending region: Brigham Young University Geology Studies, v. 42, part II, p. 235-277.



- Suppe, John, and Medwedeff, D.A., 1990, Geometry and kinematics of fault-propagation folding: *Eclogae Helveticae*, v. 83, p. 409-454.
- Taylor, J.R., 1982, An introduction to error analysis – The study of uncertainties in physical measurements: Mill Valley, California, University Science Books, 270 p.
- Taylor, W.J., 1993, Stratigraphic and lithologic analysis of the Claron Formation in southwestern Utah: Utah Geological Survey Miscellaneous Publication 93-1, 52 p.
- Threet, R.L., 1963, Structure of the Colorado Plateau margin near Cedar City, Utah, *in* Heylman, E.B., editor, Guidebook to the geology of southwestern Utah -- Transition between the Basin-Range and Colorado Plateau provinces: Salt Lake City, Intermountain Association of Petroleum Geologists 12th Annual Field Conference, p.109-117.
- Utah Governor's Office of Planning and Budget, 2000, demographic data online: <http://www.governor.state.ut.us/dea/Profiles>, accessed August 27, 2001.
- van Kooten, G.K., 1988, Structure and hydrocarbon potential beneath the Iron Springs laccolith, southwestern Utah: Geological Society of America Bulletin, v. 100, p. 1,533-1,540.
- Watson, R.A., 1968, Structural development of the Toquerville-Pintura segment of the Hurricane Cliffs, Utah: Brigham Young University Geology Studies, v. 15, part 1, p. 67-76.
- Willis, G.C., 1999, The Utah thrust system - an overview, *in* Spangler, L.E., and Allen, C.J., editors, Geology of northern Utah and vicinity: Utah Geological Association Publication 27, p. 1-9.
- Willis, G.C., Doelling, H.H., Solomon, B.J., and Sable, E.G., 2002, Interim geologic map of the Springdale West quadrangle, Washington County, Utah: Utah Geological Survey Open-File Report 394, scale 1:24,000.
- Willis, G.C., and Biek, R.F., in press, Quaternary incision rates of the Colorado River and major tributaries in the Colorado Plateau, Utah, *in* Young, R.A., editor, The Colorado River - origin and evolution: Grand Canyon Association Monograph.
- Willis, G.C., Biek, R.F., and Higgins, J.M., 1999, New  $^{40}\text{Ar}/^{39}\text{Ar}$  ages of basalt flows in the lower Virgin River basin of southwest Utah - implications for volcanic, faulting, and downcutting histories [abs.]: Geological Society of America Abstracts with Programs, v. 33, no. 4, p. A-61.
- Willis, G.C., and Higgins, J.M., 1995, Interim geologic map of the Washington quadrangle, Washington County, Utah: Utah Geological Survey Open-File Report 324, 108 p., 2 plates, scale 1:24,000.
- Willis, G.C., and Hylland, M.D., 2002, Interim geologic map of The Guardian Angels quadrangle, Washington County, Utah: Utah Geological Survey Open-File Report 395, scale 1:24,000.



## APPENDIX

### *Radiometric ages for basalt samples AC-1 and ACG-1*

#### Introduction

In this appendix we report radiometric-age data for two whole-rock samples of Quaternary basalt in the Pintura quadrangle. Lund and Everitt (1998) reported the ages, but not the analytical data, for these samples. The New Mexico Geochronology Research Laboratory (NMGRl) in Socorro, New Mexico, performed the analyses on samples provided by W.R. Lund of the Utah Geological Survey. The methods, descriptions, interpretations, data tables, and diagrams presented below are reproduced from reports submitted by the NMGRl to Lund and Ben Everitt of the Utah Division of Water Rights. The two reports had slightly different formats, reflected in the sections below.

#### Sample AC-1

##### Summary

Results for sample AC-1 were reported to Everitt by Lisa Peters of the NMGRl on June 10, 1998. The interpreted age for a groundmass concentrate sample is  $0.84 \pm 0.03$  Ma from a nearly concordant age spectrum with ~96% of the  $^{39}\text{Ar}_K$  released to define the plateau.

##### Methods

The basalt samples were crushed, sieved, treated with HCl, washed in distilled water and hand-picked to remove phenocrysts, alteration, and other extraneous material. The groundmass concentrates were then placed in machined Al discs along with interlaboratory standard Fish Canyon Tuff (Age = 27.84 Ma) as the neutron flux monitor. After sealing stacked Al discs in an evacuated quartz tube, samples and monitors were irradiated for 3 hours (N-83) in the L-67 position of the Ford Reactor at the Phoenix Memorial Laboratory, Ann Arbor, Michigan.

Following irradiation, samples and monitors were placed within an automated ultra-high vacuum extraction system where they were heated using resistance-furnace or laser methods to extract argon. Individual crystals of monitor sanidine were placed in a copper planchet and fused with a 10W Synrad CO<sub>2</sub> continuous laser. Evolved gases were purified of reactive species for two minutes using two GP-50 SAES getters, one operated at ~450°C, the other operated cold. The groundmass concentrates were step-heated in a double-vacuum Mo resistance furnace. Evolved gases were purified during heating with a SAES GP-50 getter operated at ~450°C for seven minutes, followed by ten minutes of cleanup using two additional GP-50 getters, one operated at ~450°C and the other operated cold. Argon isotopic compositions were analyzed by a MAP 215-50 mass spectrometer operated in static mode. Argon isotopes were detected by an electron multiplier with an overall sensitivity of about  $1 \times 10^{-6}$  moles/pA for the furnace. Extraction systems and mass spectrometer blanks and backgrounds were measured numerous times throughout the course of the analyses. Typical furnace blanks [were] 2 to  $5 \times 10^{-18}$  moles at masses 40, 39, 38, 37, and 36. J-factors were determined to a precision of  $\pm 0.1\%$  ( $2\sigma$ ) by analyzing 4 single crystal aliquots from each of 6 radial positions around the irradiation vessel. Correction factors for interfering nuclear reactions were determined using K- and Ca-rich glasses and salts (Table A.1). The reported ages are calculated by using the inverse variance as the weighting scheme and the errors are calculated using the method of Samson and Alexander (1987). All errors are reported at the two-sigma confidence level. The decay constant and isotopic abundances are those suggested by Steiger and Jäger (1977).

##### Results

Results are detailed in Table A.1 and are presented graphically in figure A.1. The furnace incremental heating data are displayed in figure A.1. The age spectrum is constructed using the assumption that trapped argon has the isotopic composition of modern atmosphere ( $^{40}\text{Ar}/^{36}\text{Ar} = 295.5$ ). Age spectra plot apparent age of each incrementally heated gas fraction versus the cumulative % $^{39}\text{Ar}_K$  released, with steps increasing in temperature from left to right. Where appropriate, other parameters for each of the heating steps are also plotted versus the cumulative % $^{39}\text{Ar}_K$  released. These auxiliary parameters, which aid interpretation of age spectra, include radiogenic yield (percent of  $^{40}\text{Ar}$  which is not atmospheric) and K/Ca (determined from measured Ca-derived  $^{37}\text{Ar}$  and K-derived  $^{39}\text{Ar}$ ). Interpretation of age spectra can be complicated due to such problems as excess argon, alteration, contamination,  $^{39}\text{Ar}$  recoil, and argon loss. An entirely or partially flat spectrum, in which apparent ages are the same within analytical error, may indicate that the sample is homogeneous with respect to K and Ar and has had a simple thermal and geological history. Some geochronologists use the term "plateau" to describe such flat age segments. Here we define "plateau" as three or more contiguous incrementally heated gas fractions that agree within error and together contain at least 50% of the total  $^{39}\text{Ar}_K$  released (Fleck and others, 1977). We calculate the "plateau age" by weighting each step on the plateau by the inverse of its variance (Samson and Alexander, 1987). This ensures that the heating steps with the lowest analytical error will dominate the final age calculation. Some inhomogeneous and/or hydrous samples such as hornblende and micas may yield relatively flat spectra that fail to meet strict plateau criteria. In these cases, a preferred age is calculated for the indicated steps using the same method used for the plateau age determinations.

#### Sample ACG-1

##### Summary

Results for sample ACG-1 were reported to Lund by Richard Esser of the NMGRl on July 5, 2000. The interpreted age for a groundmass concentrate sample is  $0.81 \pm 0.10$  Ma from a nearly concordant age spectrum with nearly 100% of the cumulative  $^{39}\text{Ar}_K$  released defining the plateau. Table A.2 describes the analytical methods, and table A.3 and figure A.2 present the results.



**Table A.1.** Furnace isotopic data for AC-1.

ID	Temp (°C)	<sup>40</sup> Ar/ <sup>39</sup> Ar	<sup>37</sup> Ar/ <sup>39</sup> Ar	<sup>36</sup> Ar/ <sup>39</sup> Ar (x 10 <sup>-3</sup> )	<sup>39</sup> Ar <sub>K</sub> (x 10 <sup>-15</sup> mol)	K/Ca	<sup>40</sup> Ar* (%)	<sup>39</sup> Ar (%)	Age (Ma)	±2σ (Ma)
<b>Ash Creek #1, C3:83,145.49 mg, groundmass, J=0.000518106, D=1.0024, NM-83, Lab#=8765-01</b>										
A	625	147.9	0.8825	500.8	2.08	0.58	0.0	0.9	-0.04	1.74
B	700	15.66	2.060	51.23	8.47	0.25	4.1	4.5	0.60	0.17
C	750	7.095	2.180	21.57	6.07	0.23	12.0	7.1	0.80	0.14
D	800	3.588	1.808	9.470	23.0	0.28	24.9	16.9	0.84	0.04
E	875	2.316	1.201	5.004	44.2	0.42	38.7	35.8	0.84	0.02
F	975	1.993	0.9438	3.770	72.1	0.54	46.0	66.6	0.86	0.01
G	1075	2.650	1.077	6.082	30.4	0.47	34.0	79.5	0.84	0.04
H	1250	16.52	2.864	53.97	33.8	0.18	4.6	94.0	0.71	0.12
I	1650	17.74	13.73	59.77	14.1	0.037	6.2	100.0	1.04	0.20
<b>total gas age</b>			n=9		234.1	0.38			0.82	0.08
<b>plateau</b>			n=7	steps C-I	223.6	0.39		95.5	0.84	0.03

Isotopic ratios corrected for blank, radioactive decay, and mass discrimination, not corrected for interfering reactions. Individual analyses show analytical error only; mean age errors also include error in J and irradiation parameters.

Analyses in italics are excluded from mean age calculations.

Correction factors:

$$(^{39}\text{Ar}/^{37}\text{Ar})_{\text{Ca}} = 0.00070 \pm 0.00005$$

$$(^{36}\text{Ar}/^{37}\text{Ar})_{\text{Ca}} = 0.00026 \pm 0.00002$$

$$(^{38}\text{Ar}/^{39}\text{Ar})_{\text{K}} = 0.0119$$

$$(^{40}\text{Ar}/^{39}\text{Ar})_{\text{K}} = 0.0340 \pm 0.0100$$

**Table A.2.** Methods for laser fusion and laser step-heating analyses.

#### **Sample preparation and irradiation:**

Samples provided by William Lund.

Groundmass concentrate prepared using standard techniques (crushing, sieving, magnetic separation, and hand-picking).

Samples packaged and irradiated in machined Al discs for 1 hour in D-3 position. Texas A&M Research Reactor.

Neutron flux monitor Fish Canyon Tuff sanidine (FC-1). Assigned age = 27.84 Ma (Deino and Potts, 1990) relative to Mmhb-1 at 520.4 Ma (Samson and Alexander, 1987).

#### **Instrumentation:**

Mass Analyzer Products 215-50 mass spectrometer on line with automated all-metal extraction system.

Bulk aliquots of groundmass concentrate were step-heated by a 50-watt CO<sub>2</sub> laser using a beam integrator lens.

Reactive gases removed during a 10 minute reaction with 2 SEAS GP-50 getters, 1 operated at ~450°C and 1 at 20°C. Gas also exposed to a W filament operated at ~2000°C and a cold finger operated at ~140°C.

#### **Analytical parameters:**

Electron multiplier sensitivity averaged 1.5 x 10<sup>-16</sup> moles/pA.

Total system blank and background averaged 478, 0.6, 0.4, 0.4, 2.3 x 10<sup>-17</sup> moles.

J-factors determined to a precision of ±0.1% by CO<sub>2</sub> laser-fusion of 4 single crystals from each of 6 radial positions around the irradiation tray.

Correction factors for interfering nuclear reactions were determined using K-glass and CaF<sub>2</sub> are as follows:

$$(^{40}\text{Ar}/^{39}\text{Ar})_{\text{K}} = 0.0002 \pm 0.0003; (^{36}\text{Ar}/^{37}\text{Ar})_{\text{Ca}} = 0.00026 \pm 0.000007; \text{ and } (^{39}\text{Ar}/^{37}\text{Ar})_{\text{Ca}} = 0.0007 \pm 0.00005.$$

#### **Age calculations:**

Weighted mean age calculated by weighting each age analysis by the inverse of the variance.

Weighted mean error calculated using the method of Taylor (1982).

Decay constants and isotopic abundances following Steiger and Jäger (1977).

All final errors reported at ±2σ, unless otherwise noted.



Table A.3. Analytical results for ACG-1 groundmass concentrates.

Table A.3. Analytical results for ACG-1 groundmass concentrates.

ID	Power (watts)	<sup>40</sup> Ar/ <sup>39</sup> Ar	<sup>37</sup> Ar/ <sup>39</sup> Ar	<sup>36</sup> Ar/ <sup>39</sup> Ar (x 10 <sup>-3</sup> )	<sup>39</sup> Ar <sub>K</sub> (x 10 <sup>-16</sup> mol)	K/Ca	<sup>40</sup> Ar* (%)	<sup>39</sup> Ar (%)	Age (Ma)	±1σ (Ma)
ACG-1, 26.39 mg groundmass, J=0.0001140±0.11%, D=1.00394±0.00121, NM-126, Lab#=51401-01										
A	† 2	12172	4.223	40709	0.016	0.12	1.2	0.1	29	912
B	3	342.0	5.688	1129.5	0.356	0.090	2.5	1.9	1.8	1.5
C	5	60.03	5.257	189.5	1.19	0.097	7.4	7.9	0.92	0.22
D	6	27.93	4.190	81.53	1.91	0.12	14.9	17.5	0.86	0.13
E	9	20.04	3.377	53.95	4.32	0.15	21.7	39.2	0.90	0.06
F	12	16.89	2.486	45.35	3.43	0.21	21.8	56.5	0.76	0.07
G	15	21.08	2.216	59.19	2.69	0.23	17.8	70.0	0.77	0.07
H	23	40.88	2.633	127.6	3.47	0.19	8.2	87.5	0.69	0.10
I	30	95.90	5.219	310.7	1.63	0.098	4.7	95.7	0.93	0.21
J	40	214.0	26.30	733.4	0.857	0.019	-0.3	100.0	-0.15	0.57
total gas age			n=10		19.9	0.16			0.82	1.76*
plateau		MSWD=1.0	n=9	steps B-J	19.9	0.16		99.9	0.81	0.10*
isochron		MSWD=1.0	n=10		<sup>40</sup> Ar/ <sup>36</sup> Ar=294±5*				0.83	0.10*

Notes:  
Isotopic ratios corrected for blank, radioactive decay, and mass discrimination, not corrected for interfering reactions.  
Individual analyses show analytical error only; plateau and total gas age errors include error in J and irradiation parameters.  
Analyses in italics are excluded from final age calculations.  
n= number of heating steps  
†= analyses excluded from weighted mean age.  
K/Ca = molar ratio calculated from reactor produced <sup>39</sup>Ar<sub>K</sub> and <sup>37</sup>Ar<sub>Ca</sub>.  
\* 2σ error  
\*\* MSWD outside of 95% confidence interval

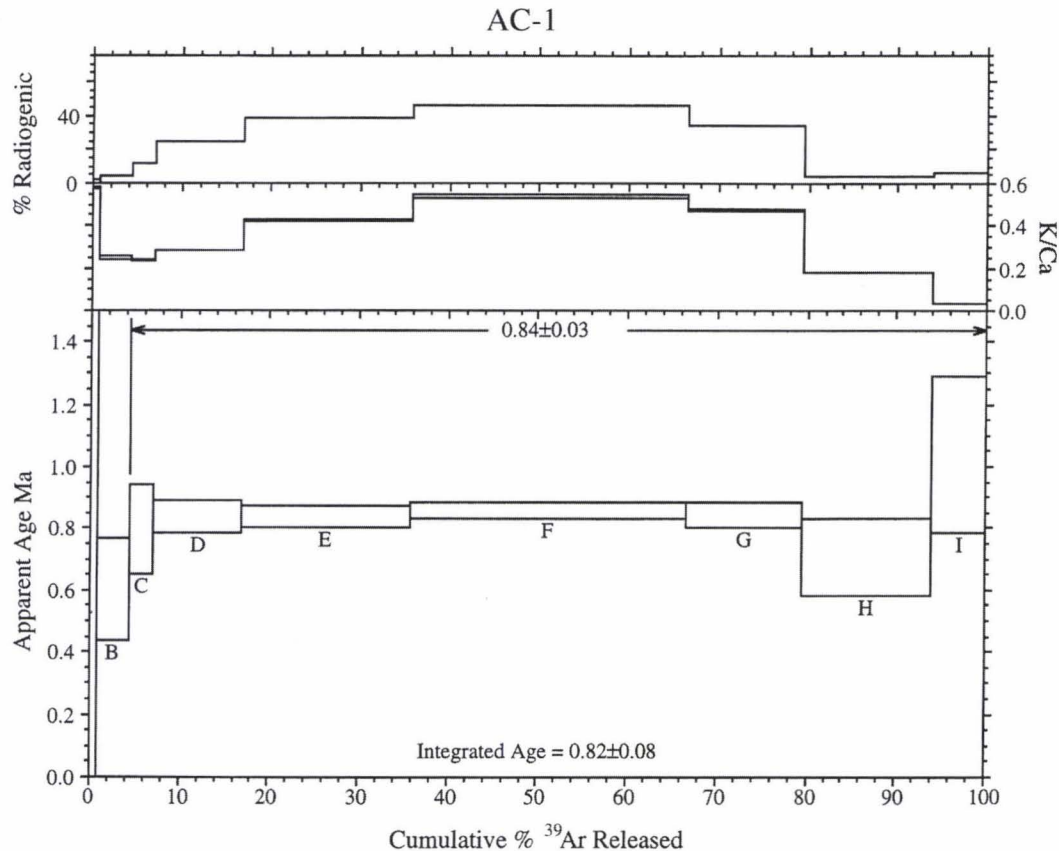
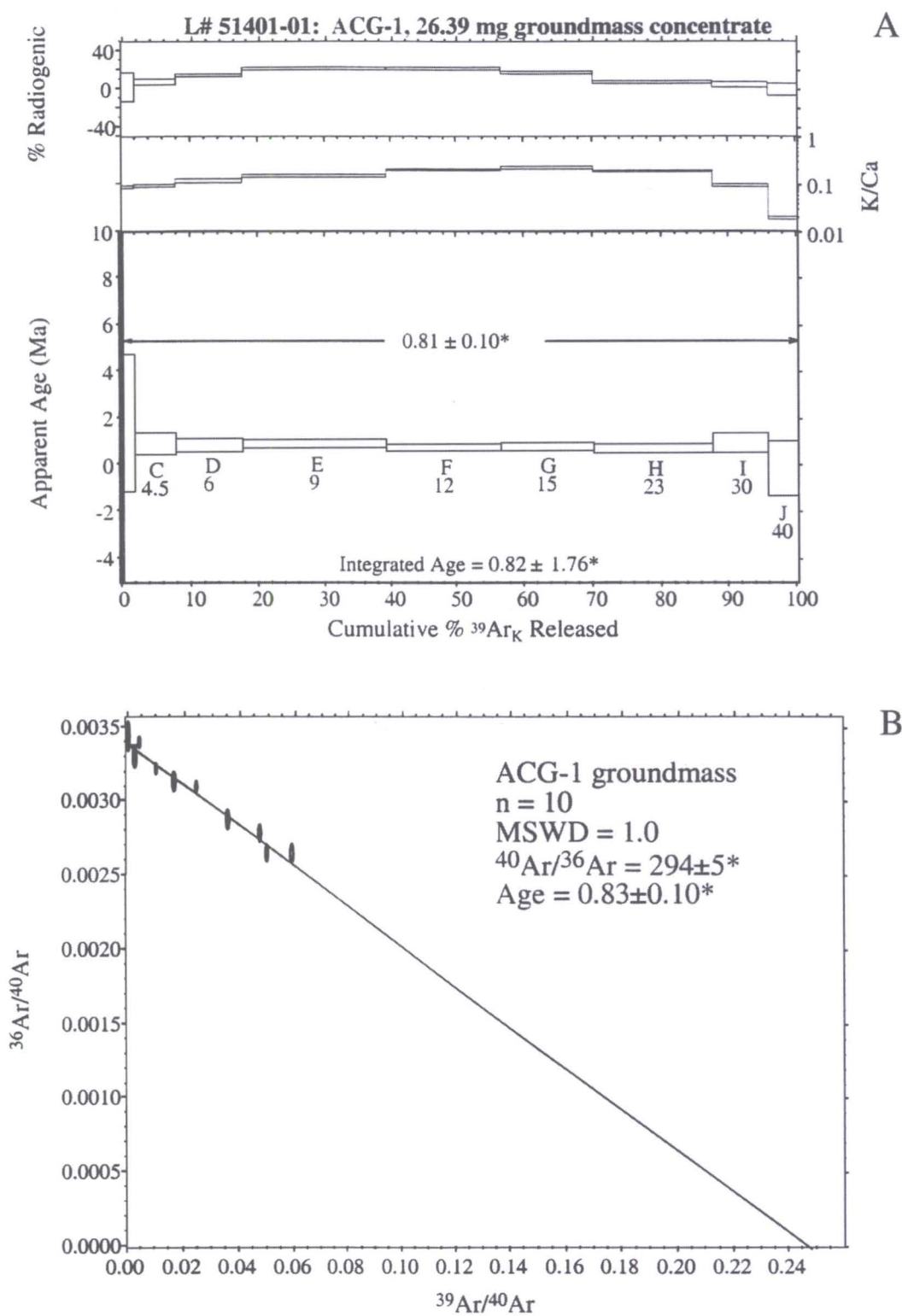


Figure A.1. <sup>40</sup>Ar/<sup>39</sup>Ar age spectrum for sample AC-1.





**Figure A.2.**  $^{40}\text{Ar}/^{39}\text{Ar}$  age spectrum and inverse isochron for groundmass concentrate ACG-1. The plateau age ( $0.81 \pm 0.10$  Ma) is the preferred age for the sample.